PROFILING BIOLOGICAL SYSTEMS WITH A CHEMICAL PROTEOMICS PROBE CARRYING A SMALL MOLECULE DRUG SCAFFOLD: APPLICATIONS TO IMMUNO-ONCOLOGY AND DRUG ALLERGY

Nadia Babaa
Faculty of Medicine and Health Sciences
Division of Experimental Medicine
McGill University, Montréal
April 2023

A thesis submitted to McGill University in partial fulfillment of the requirements of the degree of a Master's of Science in Experimental Medicine.

TABLE OF CONTENTS

ABSTRACT	5
RÉSUMÉ	7
ACKNOWLEDGMENTS	9
CONTRIBUTION OF AUTHORS	10
LIST OF FIGURES AND TABLES	11
LIST OF ABBREVIATIONS	13
CHAPTER 1: INTRODUCTION	16
FOREWARD	16
PREFACE	16
ACTIVITY-BASED PROTEIN PROFILING APPROACH	17
Biorthogonal Synthesis of Chemical Probes	18
IMMUNO-ONCOLOGY	19
Exploitation of PD-1/PD-L1 Signaling by Cancer Cells	19
Immunotherapeutic Intervention	21
Clinical Limitations of Antagonistic Monoclonal Antibodies	23
Small Molecule Inhibitors of PD-1/PD-L1 Signaling	23
BMS-202	24
BMS-202 Inhibition of PD-I/PD-L1 Binding	24
BMS-202 Antitumor Activity	26
Role of BMS-202 in Drug Discovery Efforts	27
SYNTHETIC LETHALITY	28
DNA Damage Response Pathways	28
Therapeutic Intervention Targeting DNA Damage Response	30
DRUG ALLERGY	33
Beta-Lactams and Mechanisms of Penicillin Allergy	33
Implications and Diagnosis of a Penicillin Allergy	37
DRUG DISCOVERY AND CLINICAL APPLICATIONS OF CHEMICAL PROBES	39
RESEARCH OBJECTIVES	40
Novel Chemical Probes Utilized in Present Study	41
Research Objectives	44

CHAPTER 2: PROFILING BIOLOGICAL SYSTEMS WITH A CHEMICAL PROBE CARRYING A SMALL MOLECULE ANTI-PD-L1 SCAFFOLD: APPLICATION TO IMMUNO-ONCOLOGY	. 47
INTRODUCTION	. 47
Combination therapies to enhance anti-cancer efficacy	. 47
Chemical probes to identify and explore combination therapies	. 47
METHODS AND MATERIALS	. 49
Chemical Probe Preparation/Drug Treatment	. 49
Homogenous Time Resolved Fluorescence (HTRF) PD-1/PD-L1 Binding Assay	. 50
Cell Culture	. 51
1. SAOS-2 Multiple Dose Exposure to BMS-202	. 51
2. SAOS-2 AF219 Treatment	. 51
Magnetic Bead Pulldown with Chemical Probe	. 51
Western Blot	. 53
Proteomic Mass Spectrometry	. 54
1. Liquid Chromatography Tandem Mass Spectrometry (LC-MS-MS)	. 54
2. Bioinformatics Analysis	. 54
Growth Inhibition Assay	. 55
Statistical Analysis	. 57
RESULTS	. 57
AF147 inhibits PD-1/PD-L1 binding more strongly than BMS-202	. 57
AF147 does not capture PD-L1 from cell lysates or serum	. 58
AF219 increases SAOS-2 PD-L1 levels over a 6-hour treatment	. 61
AF147 captures cell lysate proteins implicated in malignancies	. 63
NU7026 does not potentiate BMS-202 activity	. 65
BMS-202 and NU7026 interact synergistically with Doxorubicin	. 67
AF147 detects change in binding profile following SAOS-2 multiple dose exposure to BMS-202	. 71
DISCUSSION	. 73
CHAPTER 3: PROFILING BIOLOGICAL SYSTEMS WITH A CHEMICAL PROBE CARRYING A BETA-LACTAM SCAFFOLD: APPLICATION TO DRUG ALLERGY	7 6
INTRODUCTION	. 76
Prevalence and Implications of a Penicillin Allergy	. 76
Open- and Closed- Beta-Lactam Ring Chemical Probes	. 77

METHODS AND MATERIALS	79
Chemical Probe Preparation	79
Magnetic Bead Pulldown with Chemical Probe	79
Western Blot	80
RESULTS	81
AF132 and AF239 capture IgE from penicillin-allergic serum	81
AF130 and AF238 maintain activity of respective reagent probe	82
DISCUSSION	83
CHAPTER 4: DISCUSSION AND CONTRIBUTION TO KNOWLEDGE	86
IMMUNO-ONCOLOGY	86
DRUG ALLERGY	90
CONCLUSION	91
REFERENCES	92
APPENDIX	103

ABSTRACT

Small molecule-based drugs are designed to bind to a primary target. However, their biological activity and toxicity are influenced by unspecific binding to secondary targets. The identification of these targets is referred to as target profiling. Chemical probes, which contain a small molecule scaffold as a warhead and a biotin tail designed to be captured with streptavidin-coated magnetic beads, can be utilized as a target profiling method. The development of target profiling tools to advance drug development, therapy combinations, and patient stratification in the areas of immuno-oncology and/or drug allergy is needed. This thesis investigates the feasibility of using chemical probes as a target profiling method to identify binding partners of BMS-202, a small molecule programmed death-ligand 1 (PD-L1) inhibitor, and ampicillin, a penicillin beta-lactam (β-lactam) antibiotic. To this end, we used three lead chemical probes: 1) AF147 to capture and identify PD-L1 and additional targets of BMS-202 and both 2) AF132 and 3) AF239 to capture βlactam specific IgE from penicillin allergic serum. AF147 demonstrated strong inhibition of PD-1/PD-L1 binding. However, it was not able to capture PD-L1 from a solution. Further data obtained with AF147 revealed a binding profile that identified DNA dependent protein kinase catalytic subunit (DNA-PKcs), a DNA double strand break repair protein, as a dominant binding partner of the BMS-202 scaffold. Based upon the rationale that BMS-202 could be a potential inhibitor of DNA-PKcs, we designed experiments to verify whether it can sensitize cancer cells to doxorubicin. The results in comparison with NU7026, a specific inhibitor of DNA-dependent protein kinase (DNA-PK), show that BMS-202 may indeed strongly sensitize cancer cells to chemotherapy. Data obtained with AF132 and AF239 demonstrated that the chemical probes can capture β-lactam specific IgE. Albeit preliminary, the data gathered with the chemical probes serves as proof-ofconcept to support the rationale that they may be used for the identification of druggable targets and as potential diagnostic tools.

RÉSUMÉ

Les médicaments à base de petites molécules sont conçus pour se lier à une cible primaire. Cependant, leur activité biologique et leur toxicité sont influencées par la liaison non spécifique à des cibles secondaires. L'identification de ces cibles est appelée profilage des cibles. Les sondes chimiques, qui contiennent un échafaudage de petites molécules comme ogive et une queue de biotine conçue pour être capturée par des billes magnétiques recouvertes de streptavidine, peuvent être utilisées comme méthode de profilage des cibles. Le développement d'outils de profilage des cibles est nécessaire pour faire progresser le développement de médicaments, les combinaisons thérapeutiques et la stratification des patients dans les domaines de l'immuno-oncologie et/ou de l'allergie aux médicaments. Cette thèse étudie la faisabilité de l'utilisation de sondes chimiques comme méthode de profilage des cibles pour identifier les partenaires de liaison du BMS-202, une petite molécule inhibitrice du ligand 1 de la mort programmée (PD-L1), et de l'ampicilline, un antibiotique bêta-lactame (β-lactame) de la pénicilline. À cette fin, nous avons utilisé trois sondes chimiques principales: 1) AF147 pour capturer et identifier PD-L1 et d'autres cibles de BMS-202 et 2) AF132 et 3) AF239 pour capturer les IgE spécifiques des β-lactamines dans le sérum allergique à la pénicilline. L'AF147 a démontré une forte inhibition de la liaison PD-1/PD-L1. Cependant, il n'a pas été en mesure de capturer PD-L1 à partir d'une solution. D'autres données obtenues avec l'AF147 ont révélé un profil de liaison qui identifie la sous-unité catalytique de la protéine kinase dépendante de l'ADN (DNA-PKcs), une protéine de réparation des cassures double brin de l'ADN, comme un partenaire de liaison dominant de l'échafaudage du BMS-202. Partant du principe que le BMS-202 pourrait être un inhibiteur potentiel de la DNA-PKcs, nous avons conçu des expériences pour vérifier s'il pouvait sensibiliser les cellules cancéreuses à la doxorubicine. Les résultats comparés à ceux du NU7026, un inhibiteur spécifique de la protéine

kinase dépendante de l'ADN (DNA-PK), montrent que le BMS-202 peut en effet sensibiliser fortement les cellules cancéreuses à la chimiothérapie. Les données obtenues avec AF132 et AF239 ont démontré que les sondes chimiques peuvent capturer les IgE spécifiques des β-lactamines. Bien que préliminaires, les données recueillies avec les sondes chimiques servent de preuve de concept pour étayer le raisonnement selon lequel elles peuvent être utilisées pour l'identification de cibles médicamenteuses et comme outils de diagnostic potentiels.

ACKNOWLEDGMENTS

I would like to express my sincerest gratitude and appreciation for my supervisor, Dr. Bertrand J. Jean-Claude, for seeing my potential as a researcher and trusting me with the opportunity to realize it. He is a model for inclusive, respectful, and trusting leadership in academia, and I am grateful for his generous support throughout my graduate studies. I often reflect on the trust he provided me with to conduct this work and the great impact it has had on my trajectory.

Secondly, I would like to thank my academic advisor, Dr. James Martin, for his continued support and friendship throughout my studies. I greatly cherish all the conversations we shared and the positive impact they had on my motivation and goals. I am also grateful to my committee members, Dr. Jean-Jacques Lebrun and Dr. Julia Burnier.

I would like to extend thanks to my lab colleague, Dr. Ana Fragas Timiraos, for her synthesis of the chemical probes used in this study and to our collaborator, Dr. Kurt Dejgaard, for his generous support and the proteomic analysis. I am also thankful to my other lab mates, Dr. Alaa Baryaan, Dr. Anaour Hafiane, Dr. Caterina Facchin, and Casey Cohen. In addition, I would like to thank Dr. Anne-Laure Larroque for her willingness to lend a helping hand whenever needed. Importantly, I would like to thank Mme. Mary Moscone for her support and assistance of our research. Likewise, I would like to thank the many personnel and trainees at the Research Institute who I had the privilege to engage with and learn from.

Also, I would like to acknowledge my siblings for their support, motivation, and love. I also want to share my deepest appreciation, respect, and gratitude for Ali, Jeanine, and Idrîs.

Finally, I dedicate this accomplishment, and all past and future accomplishments, to my parents.

CONTRIBUTION OF AUTHORS

I wrote the thesis with the generous support and editorial help of my supervisor, Dr. Bertrand J. Jean-Claude. I also contributed to the experimental design and carried out the experimental work and analysis of all the biological experiments using the chemical probes described in this thesis. The synthesis and methodology to develop the chemicals probes were achieved by the medicinal chemistry postdoctoral fellow, Dr. Ana Belen Fraga Timiraos. The control probe was synthesized by a recent graduate, Dr. Alaa Baryyan. We are grateful to Dr. Kurt Dejgaard, Director of the Mass Spectrometry Platform of the Department of Biochemistry, for the proteomic bioinformatics, analysis, and interpretation.

LIST OF FIGURES AND TABLES

- Figure 1: Illustration of immune activity restoration through anti-PD-1 or anti-PD-L1 mAbs.
- Figure 2: BMS-202.
- Figure 3: BMS-202 crystallized with PD-L1 dimer.
- Figure 4: Illustration of synthetic lethality.
- Figure 5: Beta-lactam antibiotic classifications.
- Figure 6: Closed and open β-lactam ring in penicillin.
- Figure 7: Diagnosing a penicillin allergy.
- Figure 8: Illustration of chemical probe components and use.
- Figure 9: Strain-promoted azide-alkyne cycloaddition reaction.
- Figure 10: Chemical probes used in study.
- Figure 11: Biorthogonal components of probes.
- Figure 12: BMS-202-equipped probe.
- Figure 13: Illustration of chemical probe pulldown.
- Figure 14: Inhibition of PD-1/PD-L1 binding by AF147.
- Figure 15: PD-L1 detection in cell lysates via western blot analysis.
- Figure 16: PD-L1 detection in serum via western blot analysis.
- Figure 17: AF219 treatment increases relative PD-L1 levels in SAOS-2 cells.
- Figure 18: Selective potency of olaparib towards V-C8 BRCA cells.
- Figure 19: NU7026 did not show potentiation of BMS-202 growth inhibition.
- Figure 20: NU7026, BMS-202 and doxorubicin sensitivity in V-C8 WT and V-C8 BRCA cells.
- Figure 21: BMS-202 synergy with doxorubicin.
- Figure 22: NU7026 synergy with doxorubicin.
- Figure 23: AF147 detects change in BMS-202 binding signature in SAOS-2 cells following their prolonged exposure to BMS-202.
- Figure 24: Closed β -lactam ring structures.
- Figure 25: Open β -lactam ring structures.
- Figure 26: IgE detection in serum via western blot analysis on chemical probe-captured proteins.
- Figure 27: Comparison of IgE detection between reagent probe and biorthogonal components via western blot analysis.

Table 1: Experimental design of growth inhibition assays to compare the effects of BMS-202 and NU7026 on the potency of doxorubicin in cancer cells.

Table 2: BMS-202 binding partners in SAOS-2 and A549 WT cells identified using proteomic mass spectrometry.

Table 3: Prominent BMS-202 binding partners implicated in different cancers and cancer-related processes.

Table S1: Proteomic analysis of SAOS-2 total spectrum count.

Table S2: Proteomic analysis of A549 WT total spectrum count.

Figures 1-27 and tables 1-3 were created using BioRender.com (BioRender, Toronto, ON, CA). Chemical structures were created with ChemDraw (PerkinElmer Informatics, Waltham, MA, USA). All figures are original except for Figure 3. Details of the modifications made to the original image can be found in the figure description.

LIST OF ABBREVIATIONS

A549 WT human lung carcinoma cell line

AAL antibiotic allergy label ABP activity-based probe

ABPP activity-based protein profiling

ADE adverse drug event
ADR adverse drug reaction
B16-F10 mouse melanoma cell line

BER base excision repair
CI combination index
DDR DNA damage response

DNA-PK DNA-dependent protein kinase

DNA-PKcs DNA dependent protein kinase catalytic subunit

DPT drug provocation test
DSB double-strand break
FDR false discovery rate

HLA human leukocyte antigen
HMGB1 high mobility group box 1
HR homologous recombination

HTRF homogenous time resolved fluorescence

IC₅₀ 50% inhibitory concentration

IFN-γ interferon gamma

irAE immune-related adverse event

LC-MS-MS liquid chromatography tandem mass spectrometry

mAb monoclonal antibody MMR mismatch repair

NAD⁺ oxidized nicotinamide adenine dinucleotide

NER nucleotide excision repair
NHEJ non-homologous end joining
NIH WT mouse fibroblast cell line
NMR nuclear magnetic resonance

OD optical density

PARP poly (ADP-ribose) polymerase PD-1 programmed cell death protein-1 PD-L1 programmed death-ligand 1 PD-L2 programmed cell death ligand-2

PEG polyethylene glycol

PF₅₀ potentiation factors at 50% growth inhibition

PVDF polyvinylidenedifluoride

RAGE receptor for advanced glycation end products

SAOS-2 human osteosarcoma cell line

SCC-3 human squamous cell carcinoma-3 cell line SPAA strain-promoted azide-alkyne cycloaddition

SRB sulforhodamine B SSB single-strand break

TIL tumor-infiltrating T-lymphocytes

TME tumor microenvironment

β-lactam beta-lactam

CHAPTER 1

CHAPTER 1: INTRODUCTION

FOREWARD

This thesis is organized in a traditional format and is in partial fulfillment of the requirements laid out by the Faculty of Medicine at McGill University for the degree of a Master's of Science in Experimental Medicine.

PREFACE

The multitargeted interaction between drugs and endogenous proteins is the means by which drugs exert their pharmacological effects. Thus, identifying the protein targets of a drug is crucial to understanding its efficacy and mechanism of action. However, this is a complex process since most drugs interact with several protein targets even in cases of target-based drug development in which a drug is designed for one particular target. This presents a pressing need for a target profiling method capable of revealing the various protein targets that drug compounds associate with. The advancement of molecular biology in the post-genomic era has led to the development of several technologies that can assist in target identification including an approach termed chemical proteomics. Chemical proteomics utilizes synthetic chemistry to create small molecule chemical probes used for target fishing and subsequent identification to understand the interactions between a drug compound and its endogenous targets. 1.2

Target profiling can assist in elucidating the mechanisms underlying several physiological processes. The processes of specific interest to this study are those that yield particular drug interactions and responses in immuno-oncology in addition to those that give rise to beta-lactam (β -lactam) antibiotic allergy. Therefore, chemical probes synthesized to those ends are effective

means of testing whether they can be used to help understand those processes. The objective of this thesis is to study the feasibility of using chemical probes as a target profiling method to identify molecular determinants that can advance diagnostics and/or therapeutics in the fields of immuno-oncology and drug allergy. An in-depth review of the principles associated with the objective and discussion will precede the rationale and approach of this study.

ACTIVITY-BASED PROTEIN PROFILING APPROACH

An activity-based protein profiling (ABPP) approach to chemical proteomics was employed in this study to synthesize chemical probes. ABPP is employed to discern the activity and mechanisms of a protein using an activity-based probe (ABP).³ ABPs consist of three parts: 1) a reactive group, or warhead, 2) a reporter tag, and 3) a linker.⁴ The warhead is an electrophilic group that covalently interacts with the active site nucleophile of its target protein.³ The probes are termed "activity-based" because the only molecules which will be labeled or identified using them are those that are in active conformation with their warheads, thus enabling a reaction.² This feature makes ABPs highly selective and therefore enables their use in complex proteomes, such as those of cell lysates or intact cells.⁴ The tag of an ABP enables purification of its targets through a pull-down assay or visualization of targets using imaging-based detection.^{3,4} Examples include biotin, which binds strongly with streptavidin in pull-down assays, or fluorescent molecules, which can be used for visualization.³ Lastly, the linker separates the warhead from the tag to reduce steric hindrance between them and to improve the accessibility of the warhead to its target.³

ABPs have been extensively used to characterize proteases and their activity.⁴ The majority of ABPs developed to profile proteases are designed to target cysteine, serine, and threonine proteases due to their nucleophilic active site, which is well suited for covalent linkage to the

electrophilic warhead of an ABP.⁴ The application of these ABPs has led to greater understanding of the role proteases play in physiological and pathological processes. For example, cysteine targeted ABPs were used to identify the active sites of cysteine proteases in the eye lens that are involved in cataract formation and to also correlate their activity level to various stages of tumorigenesis.⁴ Similarly, serine targeted ABPs have been used to profile serine protease activity in different stages of breast cancer.⁴ ABPs have also been employed to study other enzyme classes and natural products with electrophilic moieties, such as β -lactam antibiotics.² Another approach to target profiling is the use of multiplexed kinase inhibitor beads that permit the capture of a broad range of kinases from biological mixtures.⁵⁻⁸

Biorthogonal Synthesis of Chemical Probes

Biorthogonal chemistry comprises chemical reactions that occur in biological environments without compromising the integrity of their molecules or processes and, thus, has been extensively applied to enhance and broaden the applications of ABPP.^{4,9} A biorthogonal reaction employs functional groups that are naturally absent from biological environments and react with one another both rapidly and selectively in physiological conditions.^{9,10} The compatibility of these types of reactions with drug molecules, along with their advancements in recent years, have made them the most commonly employed strategy to identify drug targets over the last decade.¹

The biorthogonal functional groups are relatively small in size and therefore have little to no influence on the intrinsic activity of the drug of interest.¹ Complementary biorthogonal groups, such as azides and alkynes or tetrazines and cyclopropanes, are incorporated into the molecule of interest as well as the linker-tag component of the probe.¹ The molecule is then able to interact more freely with a proteome without interference from the linker-tag portion of the probe, which

is eventually added to the proteome to allow for target capture through the reaction of the biorthogonal groups.¹

Probes synthesized using biorthogonal groups have successfully been used to identify multiple protein targets with which naturally derived drug molecules interact and to understand their implications on drug activity and mechanism of action. One example includes the use of a probe to target profile artemisinin, a potent anti-malaria drug. An alkyne was incorporated into an analogue of artemisinin and then incubated with malaria-infected red blood cells. Likewise, an azide was incorporated into a biotin tag and then added to the mixture to initiate the biorthogonal reaction between the alkyne and azide. A streptavidin enabled pull-down was completed, and the binding partners were identified via mass spectroscopy; the results indicated that the drug kills malaria parasites through broadly targeting several of their essential biochemical processes. Such demonstrations of the successful ways in which biorthogonal reactions can enhance the use of a probe supported their use in the synthesis of the chemical probes used in this study. The probes and their synthesis are presented after a review of topics pertinent to their application.

IMMUNO-ONCOLOGY

The main chapter of this study covers the use of a chemical probe used to explore proteins and mechanisms related to immuno-oncology. The upcoming sections present a review of topics relevant to its activity and findings.

Exploitation of PD-1/PD-L1 Signaling by Cancer Cells

Greater understanding of the interplay between tumor cells and the host immune system have fueled remarkable advancements in the field of cancer immunotherapy. The ability of cancer cells to evade the immune system is seen as one of the hallmarks of cancer and is carried out through a "cancer immunoediting" process. ¹² This form of immunomodulation encompasses three phases: elimination, equilibrium, and escape. ¹² Elimination occurs when innate and adaptive immune responses remove cancerous cells that appear within the host. Surviving cancer cells then mutate through a selection process favoring less immunogenicity in the equilibrium phase. This allows them to begin the last phase in the cancer immunoediting process in which the cancer cells can now escape detection and removal by the immune system. The cancer cells are then able to amplify in an unregulated manner and eventually cause noticeable symptoms or form clinically detectable tumors. ¹²

The role that the cancer immunoediting process plays in both cancer initiation and progression makes it an appealing and promising point for therapeutic intervention. Research into this process has identified programmed cell death protein-1 (PD-1) and its ligand, programmed death-ligand 1 (PD-L1), as key players in the equilibrium and escape phases. Expression of PD-1, a 288-amino acid transmembrane glycoprotein receptor, is induced on T-cells after their exposure to antigens. PD-L1 is a 290 amino acid protein receptor constitutively expressed on several immune cells as well as endothelial cells. Programmed cell death ligand-2 (PD-L2) is another ligand of PD-1, however current research primarily focuses on the role of PD-L1 since PD-L2 expression is less understood and also largely restricted to antigen presenting cells. Upon ligation in normal physiological conditions, PD-1/PD-L1 signaling acts as an immune checkpoint that serves to avoid autoimmunity and induce peripheral tolerance by down-regulating T-cell activation.

The vital role the PD-1/PD-L1 pathway plays in healthy immune regulation offers cancer cells an opportunity to exploit normal cellular processes to evade immune detection and removal.

High mobility group box 1 (HMGB1) is a gene expression regulator normally found in the nucleus but can be secreted into the extracellular matrix where it can play a significant role in cancer pathogenesis. HMGB1 is abundant in the tumor microenvironment (TME) of many solid tumors and can bind to the receptor for advanced glycation end products (RAGE), which is a multiligand binding transmembrane protein involved in several inflammatory diseases. RAGE activation by HMGB1 activates several oncogenic pathways including the transcription of PD-L1 by cancer cells to induce immunosuppression of the TME. 15,16

It has been observed that several types of tumor cells express PD-L1, and their subsequent ligation with PD-1⁺ tumor-infiltrating T-lymphocytes (TILs) in the TME is believed to suppress antitumor immune activity.¹³ In the example of human melanoma, PD-1⁺ TILs show impaired cytokine production when compared with PD-1⁻ TILs.¹³ PD-1/PD-L1 signaling in the TME helps tumor cells create a state of resistance to immune activity through T-cell exhaustion.^{13,14} This allows cancer cells to enter the escape phase of the immunoediting process and thereby proliferate within their host.

Immunotherapeutic Intervention

A large body of evidence supports that the disruption of PD-1/PD-L1 signaling within the TME promotes antitumor immunity and offers the potential for targeted anti-cancer therapeutics.¹⁷ This has led to the clinical approval of six antagonistic monoclonal antibodies (mAbs) against either PD-1 or PD-L1: nivolumab, pembrolizumab, cemiplimab, atezolizumab, avelumab, and durvalumab.¹⁸ These mAbs have shown promising clinical responses in advanced solid and hematologic malignancies including reduction in tumor size, longer overall survival, and longer duration of response for patients and are also less toxic than traditional cytotoxic chemotherapies.¹⁹

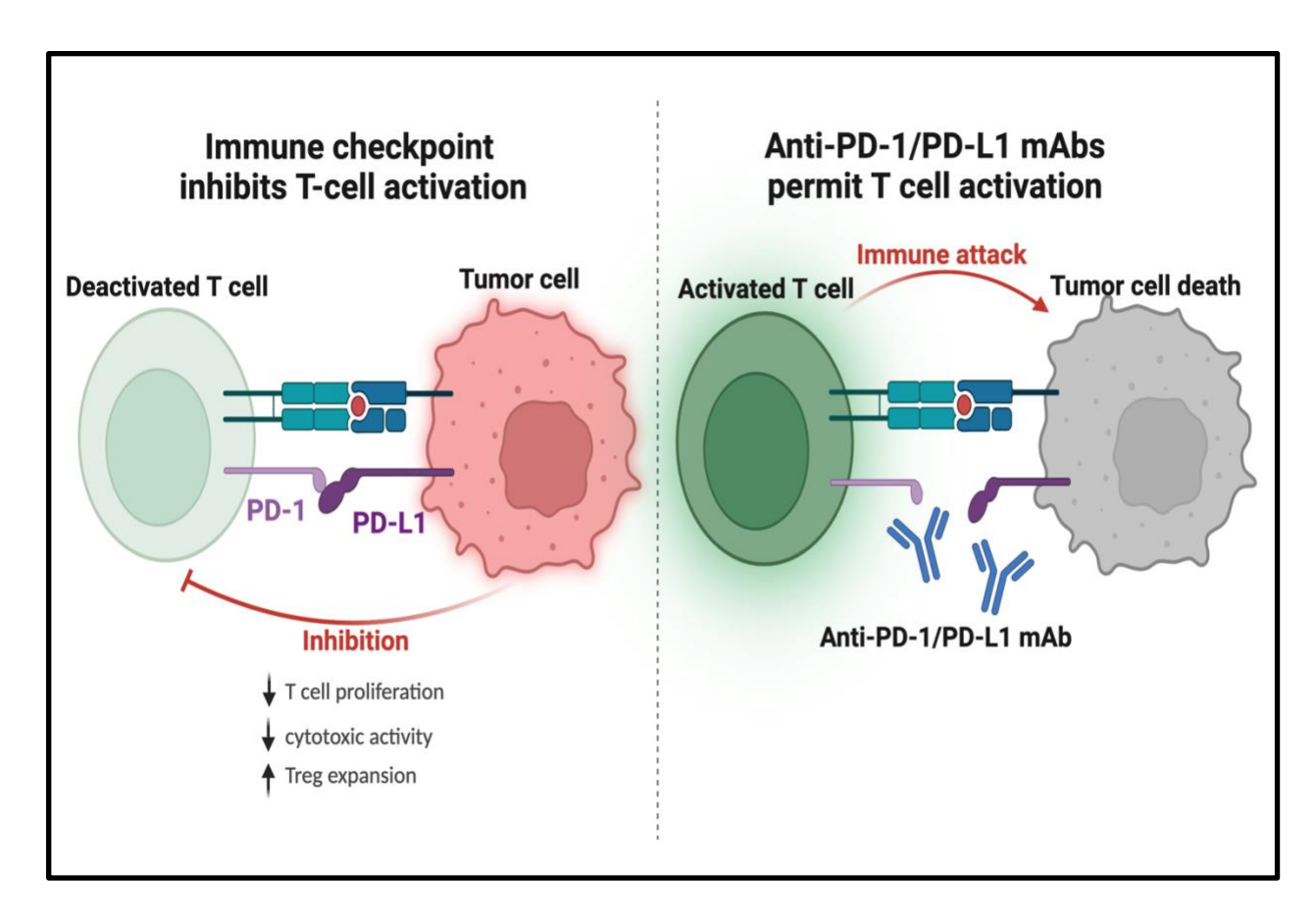


Figure 1: Illustration of immune activity restoration through anti-PD-1 or anti-PD-L1 mAbs. Tumor cells create a state of resistance to immune activity through T-cell exhaustion via T-cell PD-1 and tumor cell PD-L1 ligation (left). The mAbs raised against either protein prevents the immune-silencing interaction and restores immune activity to the TME (right). The material restores immune activity to the TME (right).

These responses can be explained by the strong pharmacodynamic profile displayed by the mAbs, which aids in interrupting the immune checkpoint pathway created by the binding of PD-1 and PD-L1. The mAbs clinically used to target PD-L1 exhibit binding affinities in the picomolar range that translate to potent inhibitory performance with 50% inhibitory concentration (IC₅₀) values also in the picomolar range.²⁰ The effectiveness of the mAbs in blocking the PD-1/PD-L1 pathway comes from their competition for the binding surface in which PD-1 and PD-L1 interact.²⁰

Clinical Limitations of Antagonistic Monoclonal Antibodies

There exist several limitations with the mAbs despite the benefits they have brought to clinical settings. One such limitation is their failure to elicit the anti-cancer immune activity in majority of the patients treated with them resulting in varied response rates across different types of cancers. ¹⁹ Another limitation is one commonly seen with biologics created to enhance the host immune system referred to as immune-related adverse events (irAEs) in which the activation of T lymphocytes causes autoimmune reactions and damage to healthy tissues. ²⁰ These reactions create a clinical problem as the treatment for them entails the use of systemic immunosuppressants, which negate the therapeutic benefit mAbs provide as immune checkpoint inhibitors. ²⁰

Small Molecule Inhibitors of PD-1/PD-L1 Signaling

The limitations of antagonistic mAbs can be addressed with the use of small molecule inhibitors. The mAbs have poor pharmacokinetic profiles with low volumes of distribution, which prevents them from reaching and penetrating the TME, and prolonged elimination half-lives, which compounds the difficulty of managing irAEs. ^{19,20} Furthermore, the mAbs present practical limitations with high administration and manufacturing costs as well as diligent and efficient storage to prevent loss of structural integrity. These factors significantly add to both patient and healthcare system expenditure. ²⁰

By contrast, the small molecules have more favorable pharmacokinetic profiles with higher volumes of distribution, which enable greater penetration of the TME, and shorter half-lives, which alleviate some difficulty in the presence of irAEs. ^{19,20} They also have higher oral bioavailability than mAbs, which eases their administration to patients, and the economic burden associated with them is significantly less on patients and the healthcare system. ²⁰

The advantages of small molecules, along with the clinical benefits seen when treating malignancies with immune checkpoint blockade, have created a need for the development of small molecule inhibitors targeting the PD-1/PD-L1 pathway. Increased structural knowledge of the PD-1/PD-L1 interaction has guided the development of several small molecules that may disrupt the pathway over the last several years.^{20,21}

Small molecule inhibitors primarily consist of peptidomimetics.²⁰ Peptides are appealing for drug discovery efforts because they have the greatest chemical diversity of all biological molecules and their conformational behavior confers favorable pharmacodynamic profiles.²² Peptidomimetics are peptide analogs that retain the structural and functional elements of peptides, which allows them to interact with endogenous targets to produce biological effects.²²

BMS-202

The chemical probe utilized for the immuno-oncology portion of this study is tethered to a scaffold derived from BMS-202, a small molecule inhibitor of the PD-1/PD-L1 pathway. Therefore, a review of BMS-202 is presented prior to the introduction of the novel chemical probe and research objectives.

BMS-202 Inhibition of PD-I/PD-L1 Binding

This study focuses on a particular peptidomimetic molecule, BMS-202, which was patented by Bistol-Myers Squibb and developed using the (2-methyl-3-biphenylyl)methanol scaffold (Figure 2).²¹ In its patent, BMS-202 was reported as inhibiting the interaction between PD-1 and PD-L1 with an IC₅₀ of 18nM.²³ It was later demonstrated that BMS-202 binds directly to PD-L1 based on a nuclear magnetic resonance (NMR) experiment that displayed significant shifts of ¹⁵N labeled

PD-L1 peaks upon its titration with BMS-202.²¹ The shifts were not observed via the same method using ¹⁵N labeled PD-1 and therefore indicate BMS-202 specificity for PD-L1.²¹ Another NMR experiment supported the claim that BMS-202 disrupts PD-1/PD-L1 binding when the shifts correlated to a PD-1/PD-L1 complex were narrowed when titrated with BMS-202, thus indicating its dissociation.²¹

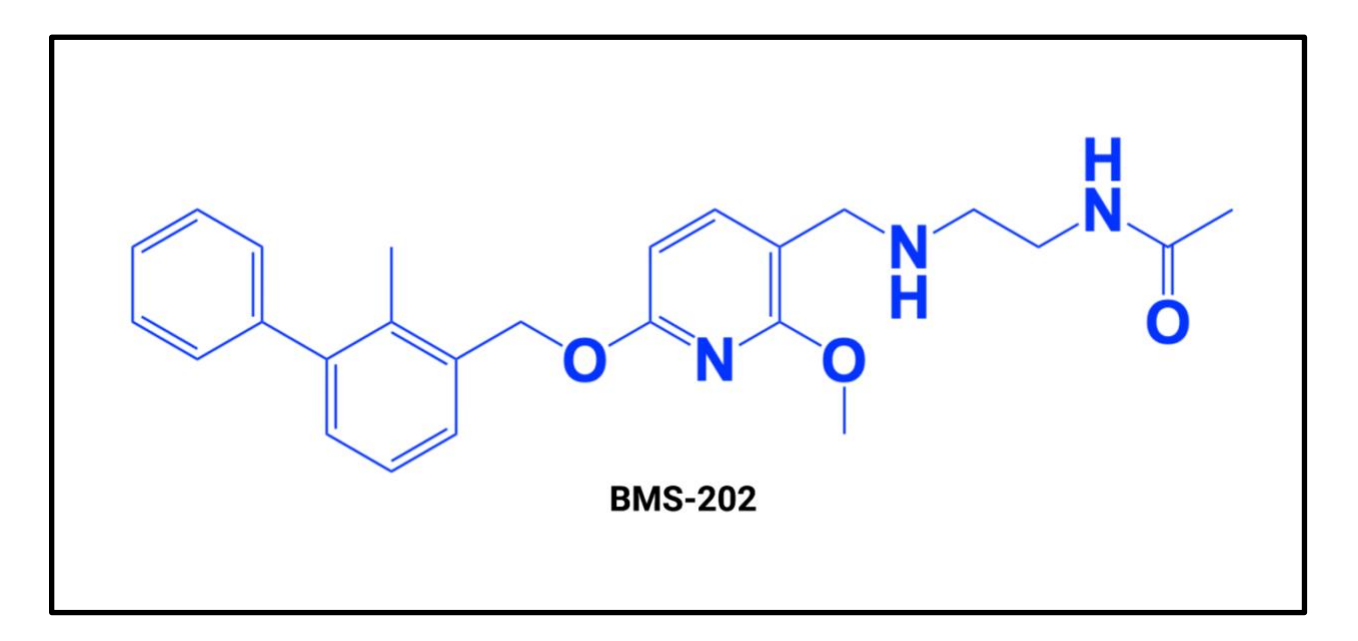


Figure 2: BMS-202. Chemical structure of BMS-202.²⁴

Crystallization of BMS-202 in a complex of PD-L1 showed that BMS-202 binds to its target in a 1:2 stoichiometric ratio with four molecules of PD-L1 organized into two dimers and one molecule of BMS-202 occupying a hydrophobic cylindrical cleft located at each dimer interface (Figure 3).^{20,21} That same area overlaps with the interaction surface in which PD-1 engages with PD-L1.²¹ Subsequent NMR experiments and size-exclusion chromatography demonstrated that BMS-202 induces PD-L1 dimerization, which further occludes the PD-1

binding site. These findings suggest a structural mechanism of action for the interference of BMS-202 with PD-1/PD-L1 binding.^{20,21}

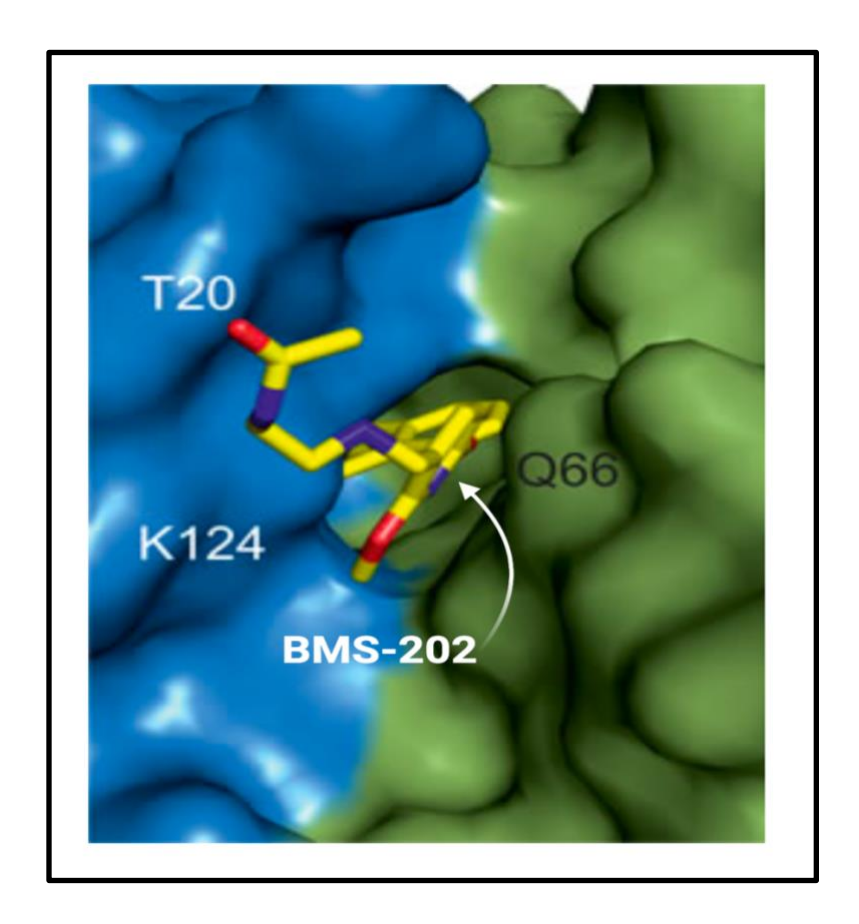


Figure 3: BMS-202 crystallized with PD-L1 dimer.²¹ BMS-202 (yellow) occupies a hydrophobic cylindrical cleft at the interface of a PD-L1 dimer (blue and green molecules). BMS-202 label (white) and arrow (white) were added to the original image.²¹

BMS-202 Antitumor Activity

Investigation into BMS-202 in vivo and in vitro activity ensued after its patent. A cytotoxic assay of BMS-202 on the mouse melanoma cell line (B16-F10) and the mouse colorectal carcinoma cell line, CT26, yielded 48hr IC50 values of 23.5 μ M and 15.3 μ M, respectively, and yielded a 72hr IC50 of 10.3 μ M against human CD3⁺ cells. ²⁵ Despite its low cytotoxicity, BMS-202 displayed its ability

to restore immune activity by significantly reversing PD-L1-mediated inhibition of interferon gamma (IFN- γ) release in human CD3⁺ T cells in vitro.²⁵

It also displayed an in vivo inhibition rate of 30.3% and 50.1% on mouse B16-F10 tumors with weights of 30 mg/kg and 60 mg/kg, respectively. Plasma IFN- γ level measures of the same tumors were significantly increased in BMS-202 treated-tumors compared to those of the control group. Flow cytometry data on the B16-F10 tumors revealed that BMS-202 induced the antitumor activity through an increase of cytotoxic activity of tumor-infiltrating CD8+ T cells, demonstrated with increased cell counts of CD8+IFN- γ + T cells, and through the inhibition of Treg expansion, demonstrated with decreased cell counts of CD4+CD25+CD127low/- T cells. 25

Another study testing BMS-202 on the human squamous cell carcinoma-3 cell line (SCC-3) also highlighted its antitumor activity. It displayed an in vitro IC₅₀ of 15uM and an in vivo inhibition rate of 41% against the SCC-3 tumors transplanted in mice.²⁴ However, the antitumor activity was not attributed towards increased immune activity within the TME since the numbers of tumor-infiltrating CD8⁺ T cells were significantly lower in the BMS-202 treated-tumors compared to those of the control group; rather, it is believed that cytotoxicity, which was displayed through notable body-weight reduction seen in the BMS-202 treated mice, played a greater role in the antitumor response than did any restored immune activity.²⁴

Role of BMS-202 in Drug Discovery Efforts

Although mainly promising, the insufficient evidence supporting a specific way in which BMS-202 produces antitumor effects is a contributing factor that has prevented it from advancing from preclinical to clinical trials. However, its preliminary studies highlight the feasibility of small molecule inhibitors to target the PD-1/PD-L1 interface. It is also noteworthy that structural

analyses of BMS-202 interacting with PD-L1 have identified surfaces and amino acid residues that are consequential to PD-1/PD-L1 binding and have encouraged research efforts directed towards improving its design to optimize its function as a therapeutic immunomodulator against cancer. BMS-202 was selected as the inhibitor scaffold of our chemical probe due to its proven affinity for PD-L1 dimers and the PD-1/PD-L1 complex.

An additional advantage of small molecule inhibitors is their feasibility to be leveraged as part of combination therapies against cancer. Combination therapies, in which chemo or immunotherapeutic medications are used in tandem or alongside modalities such as surgery and radiation, are currently being designed and clinically tested to increase and prolong treatment responses among more patients.^{19,27} The favorable pharmacokinetic profiles, manufacturing costs, and easier administration associated with small molecules inhibitors make them more suitable to combination therapies than mAbs.¹⁹

SYNTHETIC LETHALITY

Given that one of the findings of our studies indicated that BMS-202 may potentially target proteins involved in DNA damage repair, a review of the pathways and proteins involved is herein presented.

DNA Damage Response Pathways

Eukaryotic cells constantly encounter both endogenous and exogenous forms of stress that threaten the integrity of their DNA. However, cells are well equipped to respond to such stressors through their sophisticated DNA damage response (DDR) pathways, which physically correct and/or remove damage to lessen its detrimental effects on the cells' genomic material.²⁸ There are five

major DNA repair pathways that are activated to correct differing types of DNA damage at various points in the cell life cycle: base excision repair (BER), nucleotide excision repair (NER), mismatch repair (MMR), homologous recombination (HR), and non-homologous end joining (NHEJ).²⁸

BER is initiated to correct damage from endogenous base lesions, abnormal bases generated from environmental stressors or endogenous metabolic intermediates, and DNA single-strand breaks (SSBs).²⁹ DNA glycosylase initiates BER by excising the damaged base and creating an abasic or AP site that either lacks a purine (apurinic site) or pyrimidine (apyrimidinic site). The AP site is further cleaved by an endonuclease to allow DNA polymerase to synthesize the appropriate complementary base. DNA ligase completes the process by sealing the DNA strand.³⁰

NER corrects more complicated DNA damage such as UV light induced bulky adducts or chemotherapeutic induced crosslinks, which would distort DNA structure if left unaddressed. ^{29,31,32} Enzymatic reactions involving over 30 proteins recognize the damage, excise it, and then repair and ligate the DNA strand. ²⁹ MMR also recognizes crosslinks but is mainly used to resolve inappropriately paired bases by DNA polymerase during DNA replication. The process consists of mismatch identification, removal, and replacement. ^{29,31}

BER, NER and MMR are carried out for SSB repair. Double-strand breaks (DSBs) are the most deleterious form of DNA damage to genome integrity and the pathways involved in their repair are NHEJ and HR.³¹ HR is referred to as an error-free pathway since it occurs during S/G₂ phase of the cell cycle when sister chromatids are present allowing DNA damage to be corrected using an undamaged homologous DNA strand.³¹ NHEJ is used throughout the entire cell cycle, but is mainly used during G₁ when the sister chromatids are not present and therefore no homologous template is available.³³ NHEJ corrects DSBs by directly ligating DNA ends, and,

although it is effective, it is an error-prone repair pathway that can give rise to genomic instability.³⁴

Therapeutic Intervention Targeting DNA Damage Response

Failure to correct DNA damage can disrupt cellular processes and functions and cause dysregulation of cell proliferation and death in a manner that promotes tumorigenesis. ^{29,31} Indeed, most cancers become deficient in a DDR pathway or function during their progression. ³⁵ Genomic instability enables the hallmarks of cancer, which consist of the advantageous and acquired characteristics of cancerous cells, such as the previously discussed feature of immune evasion. ¹² Similar to the way in which the exploitation of the PD-1/PD-L1 pathway by cancer cells provides an appealing opportunity for therapeutic intervention, altered DDR proteins and pathways within cancer cells has led to several targeted therapies that leverage the mutations in a therapeutic manner. ^{12,17}

One such example is the approach referred to as synthetic lethality. The concept was originally described through studying the genetics of a drosophila population; two genes, or groups of genes, that are viable when separated but lethal in combination were termed synthetically lethal to each other.³⁶ In the case of cancer, deficiency in DDR can result in the dependence of a cancer cell on a compensatory pathway for its own survival.³⁵ This provides an opportunity for pharmacological intervention to elicit lethality by employing an inhibitor of the compensatory pathway. This approach is preferential to cancerous cells through its target of their synthetically lethal protein and is therefore less cytotoxic than traditional chemotherapeutic agents.²⁹

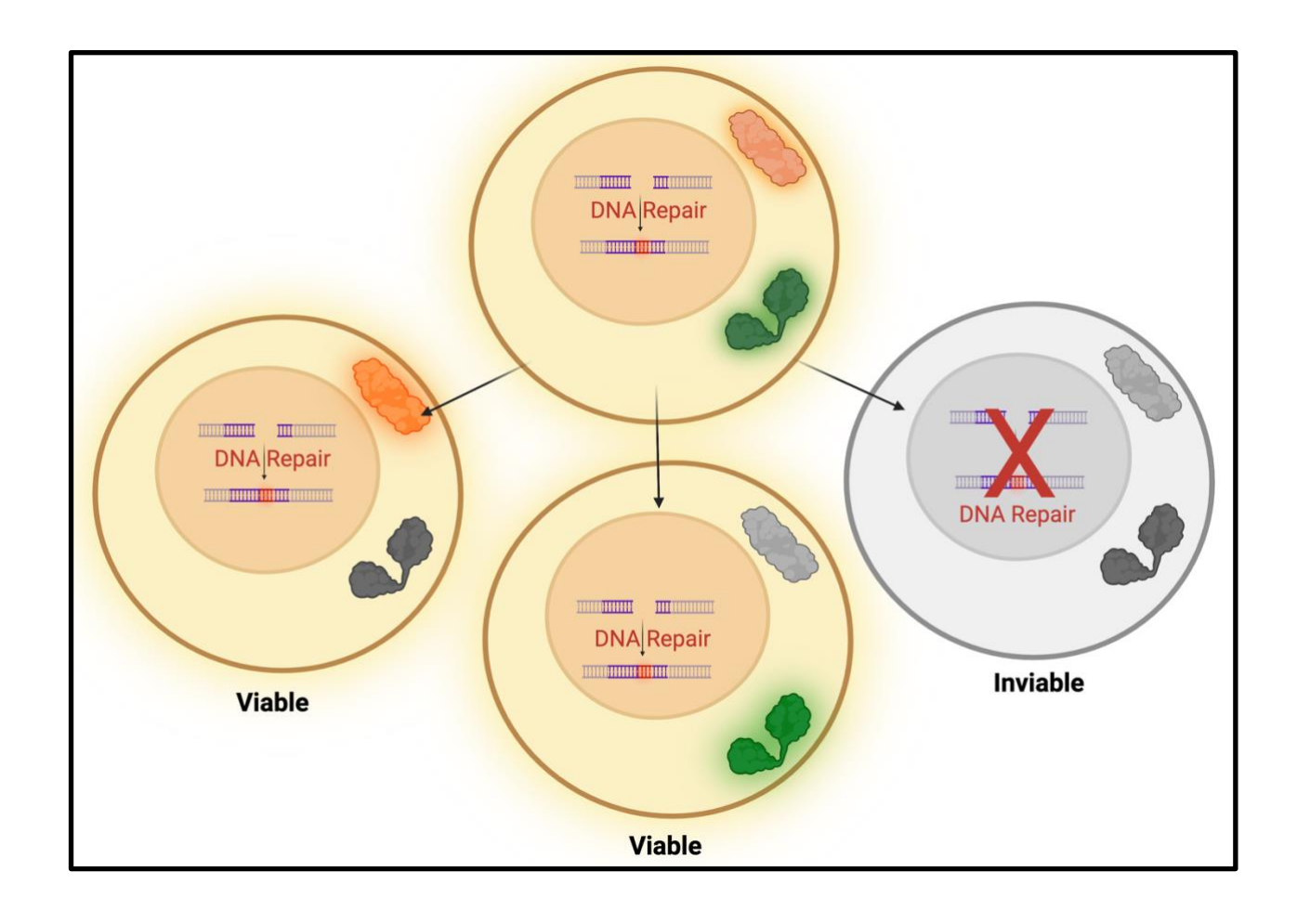


Figure 4: Illustration of synthetic lethality. Three pathways are shown for a healthy cell with two DDR proteins (top) to illustrate synthetic lethality. In the first and second pathways (bottom left and middle), one of the DDR proteins is deficient but the cell remains viable due to the compensatory DDR of the second protein. In the third pathway (bottom right), both DDR proteins are deficient so DDR cannot proceed, and the cell becomes inviable. Synthetic lethality can be pharmacologically induced to target the compensatory DDR protein to induce cell death.^{29,35}

An example that highlights the therapeutic opportunity of synthetic lethality is the use of poly (ADP-ribose) polymerase (PARP) inhibitors in tumors deficient in HR.²⁹ PARP consists of a family of 17 proteins that assist in several essential processes within the cell such as DNA repair, stress response, and apoptosis.³⁴ PARP1, the most characterized PARP protein, is a major

component in DNA repair of SSBs through BER.³⁴ It acts as a critical SSB sensor protein that rapidly binds to DNA for repair and resealing. PARP1 utilizes oxidized nicotinamide adenine dinucleotide (NAD+) as a substrate for itself and other proteins involved in its catalytic response.³⁷ PARP inhibitors compete for NAD+ leaving PARP1 inactivated and trapped on DNA.³⁵ PARP-DNA complexes can generate genotoxic DSBs through their blockade of the DNA replication fork.³⁵ As previously mentioned, DSBs detected during the S phase, or the DNA replication phase of the cell cycle, are repaired by HR.³¹ However, a tumor deficient in HR will be unable to repair the damage caused by PARP inhibition and eventual cell death will occur.³⁴

The tumor suppressor genes BRCA1 and BRCA2 are associated with breast and ovarian cancers, two well-known examples of HR deficient tumors well suited for synthetic lethality.³⁵ RAD51 is a critical strand-exchange protein that catalyzes the HR defining events of homology search as well as strand invasion and exchange.³⁸ BRCA1 and BRCA2 colocalize with RAD51 and activate its DSB repair activity making them crucial players in HR.³⁹ Consequently, their loss of function contributes to genomic instability and is correlated to a significant increase in cancer risk for individuals with germline BRCA mutations.³⁵ However, the HR deficient cancers are candidates for targeted and synthetically lethal PARP inhibition.³⁴

PARP inhibitors such as olaparib, which is approved for use in a few DDR deficient cancers, have demonstrated the effectiveness of this strategy through their selective and wide therapeutic window for BRCA-deficient cells.^{31,35} This has encouraged research aimed at defining other synthetically lethal interactions that can be exploited therapeutically using DDR agents. An example of critical importance to the contents of this thesis incudes research involving inhibitors of DNA-dependent protein kinase (DNA-PK). DNA-PK is an essential enzyme in NHEJ comprised of DNA-PK catalytic subunits (DNA-PKcs) and the heterodimeric regulatory complex,

Ku.⁴⁰ DNA-PK inhibitors are actively being investigated for their synthetic lethality with other genetically or pharmacologically induced DDR deficiencies.^{41,42}

Targeting DDR may also intervene with the development of resistance to commonly used forms of chemo- and radiotherapies. These therapies carry out their anti-cancer activity through their cytotoxic generation of DSBs. However, one mechanism that may confer their resistance is cancer cell repair of DNA DSBs through pathways such as HR and NHEJ.^{32,43} This is believed to contribute to doxorubicin resistance, a chemotherapy that targets DNA topoisomerase II and induces DSB.⁴⁴ Targeting key proteins involved in HR or NHEJ, such as DNA-PK, is therefore a potential therapeutic strategy to impede that process and augment anti-cancer efficacy.^{43,44}

DRUG ALLERGY

Two chemical probes in this study were used to explore drug allergy. A review of penicillin allergy is introduced prior to the presentation of the results and discussion yielded from their experimentation.

Beta-Lactams and Mechanisms of Penicillin Allergy

β-lactams antibiotics are bactericidal agents that interrupt cell-wall formation in gram-negative and -positive bacteria. They are the first choice and most widely used antibiotics and consist of penicillins, cephalosporins, monobactams and carbapenems. All β-lactams share a core, β-lactam ring with structural differences seen in their adjacent rings and R-group side chains (Figure 5). Sensitization to the β-lactam ring and/or the side chains can lead to allergic responses.

Figure 5: Beta-lactam antibiotic classifications. Chemical structures of penicillins, cephalosporins, monobactams, and carbapenems. β-lactam ring is highlighted in red.⁴⁶

Penicillin allergies are the most prevalent among β-lactams and cross-reactivity between them and other classes is rare and not considered clinically significant.⁴⁸ The thiazolidine ring and lack of additional side-chains is unique to penicillins.^{46,49} Its β-lactam ring is highly strained, and its opening by nucleophilic attacks of free amino groups of endogenous proteins is an efficient process that forms the penicilloyl metabolite.⁵⁰ The penicilloyl metabolite is considered an

antigenic intermediate since it readily links to bodily proteins and forms complexes that are believed to elicit an immune reaction.⁵¹ In fact, penicilloyl accounts for up to 95% of penicillin bound to tissue, making it a major determinant of an allergic reaction whereas the parent penicillin with a closed β-lactam ring is considered a minor determinant (Figure 6).^{49,51}

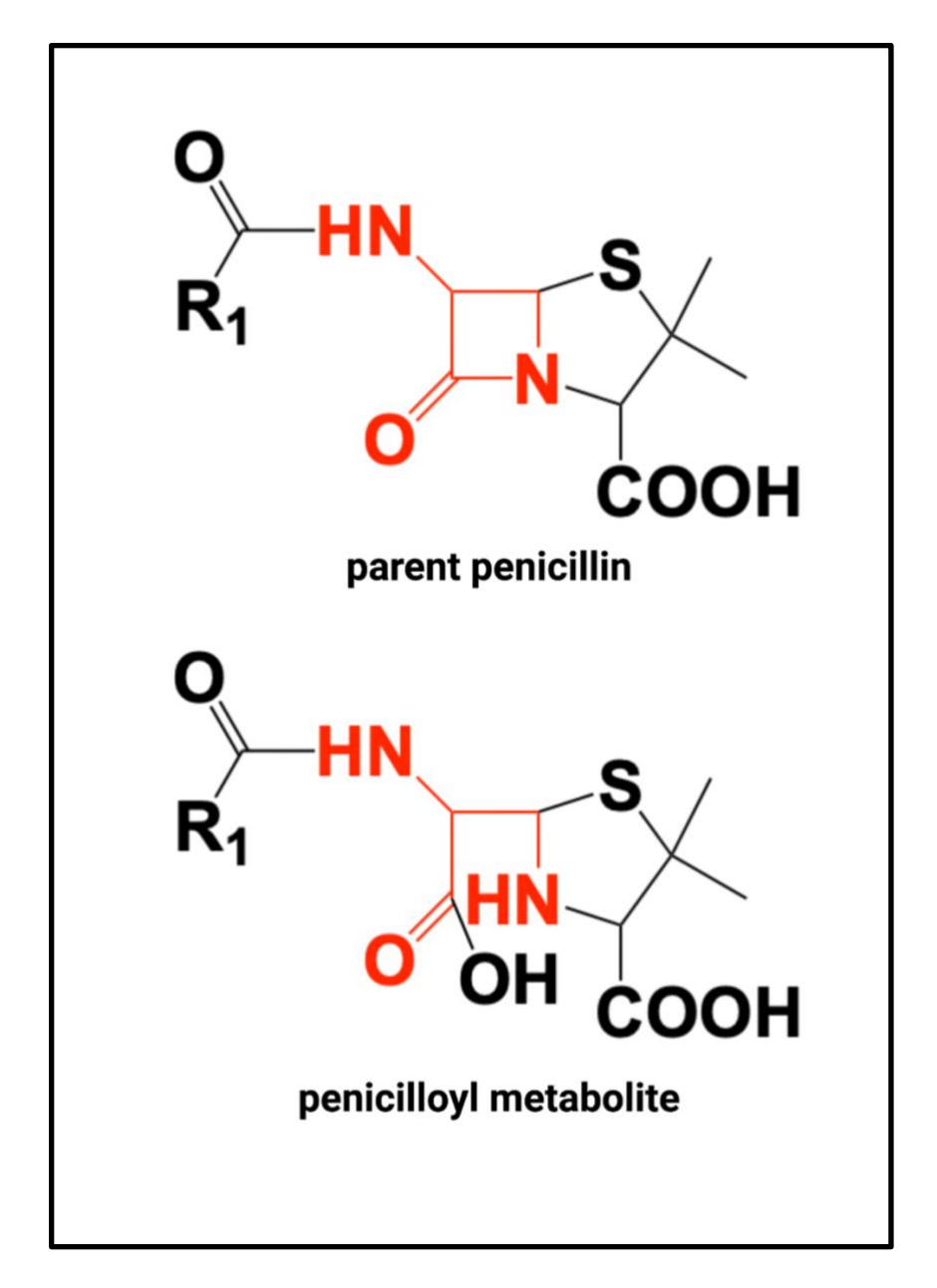


Figure 6: Closed and open β-lactam ring in penicillin. Chemical structure of parent penicillin and its penicilloyl metabolite.⁵²

Antibiotic allergies encompass a diverse set of adverse drug reactions (ADRs), which are either non-immune mediated Type A reactions or immune mediated Type B reactions.⁵³ More than 80% of all ADRs are considered Type A and are driven by intolerance due to drug pharmacological properties, whereas Type B reactions are less predictable based on such information.⁴⁷ Drug hypersensitivity encompasses both Type A and B ADRs while drug allergy describes Type B reactions and the immune responses they elicit.⁴⁶

Type B reactions are divided into four pathophysiological types based on their mediators, manifestations and severity according to the Coombs and Gell model: immediate IgE mediated type 1 reactions, IgG or IgM mediated type 2 reactions, immune complex mediated type 3 reactions, and delayed T-cell mediated type 4 reactions. Delayed type 4 reactions are the ones most frequently seen with penicillins while immediate type 1 reactions are rare. IgE mediated type 1 reactions are of specific interest for the purposes of this study.

It is hypothesized that Type B reactions arise from specific interactions between the causative agent and the specific human leukocyte antigen (HLA) alleles.⁵⁵ HLA alleles are part of the major histocompatibility complex, or MHC, locus and are associated with stimulating an immune response to external antigens.⁵⁶ Immunogenic complexes that give rise to such a response through binding to T cell receptors are formed from an HLA allele, a peptide ligand of the HLA, and the causative agent or drug molecule.⁵⁵

Different mechanisms have been proposed to explain how HLA molecules activate the immune system, and the one that best supports the events of an IgE mediated type 1 reaction to antibiotics is the hapten model.^{55,57} This mechanism describes the antibiotic molecule as a hapten that covalently binds to a peptide ligand of an HLA to form a large immunogenic hapten-carrier complex.⁵⁷ The complexes act as antigens that bind to and are internalized by dendritic cells for

presentation to naïve CD4⁺ T cells.⁴⁹ These cells subsequently develop into type 2 helper T cells and produce interleukin-4 and -13 leading to the differentiation of B cells into plasma cells that secrete antibiotic-specific IgE antibodies. Basophils and mast cells recognize the IgE antibodies, causing them to degranulate and release soluble inflammatory mediators, such as histamine, which drive the rapid anaphylactic symptoms of the IgE mediated allergic response.⁴⁹ Antibiotics are among the classes of drugs most reported to trigger anaphylaxis.⁵⁸ Importantly, penicillins cause the most fatal and non-fatal anaphylaxis among all drug-induced reactions in the United States and the United Kingdom.⁴⁹

Implications and Diagnosis of a Penicillin Allergy

Patient-reported antibiotic allergy labels (AALs) are highly prevalent and can negatively impact appropriate use of antibiotics and patient health outcomes.⁵⁹ The Canadian Society of Allergy and Clinical Immunology as well as the United States Centers of Disease Control and Prevention report that although about 10% of the population carries a penicillin AAL, up to 98% of this group can in fact tolerate these antibiotics upon further assessment.^{46,60} Misuse of an AAL has several individual and public health implications including increased use of suboptimal second-line or broader-coverage and more costly antimicrobials, increased adverse drug events (ADEs), more postoperative surgical-site infections, increased risk of antibiotic resistance, and higher healthcare costs resulting from longer hospital stays.^{46,49}

Patients may carry a penicillin AAL due to a suspected reaction that was misclassified during childhood.⁴⁶ Importantly, there is strong evidence supporting that sensitization to penicillin is lost with time.⁴⁹ This provides the rationale for penicillin allergy delabeling, which is a

procedure for thoroughly assessing the validity of a label and removing it if appropriate, as active intervention to lessen the erroneous avoidance of penicillins.⁶¹

Clinical diagnostic tools for antibiotic allergy typically include history of drug hypersensitivity, skin testing, and the gold standard drug provocation test (DPT). 46,48 In vitro assessments to diagnose a β -lactam allergy are not well established clinically. 46 Skin testing is regularly used but has poor predictive value, and it has been observed that many skin-test positive patients have negative oral DPTs, and are therefore not clinically allergic. 46,48 DPTs present their own challenges such as the lack of standardized protocols for the assessment, the risk patients may assume when tested, and the need for trained personnel and specialized settings to conduct the test. 62,63 Recent guidelines suggest the use of one or both tests based on stratification of patients into low, intermediate, and high risk of ADRs as the safest and most effective way of evaluating their AAL (Figure 7). 46,49 There is a need for studies and tools that can help in risk stratification guidelines to increase the safety and accuracy of delabeling. 64 One purpose of this thesis is to explore the use of chemical probes tethered to a β -lactam scaffold as tools that can be used to assist in risk stratification by determining the binding profile of β -lactam antibiotics.

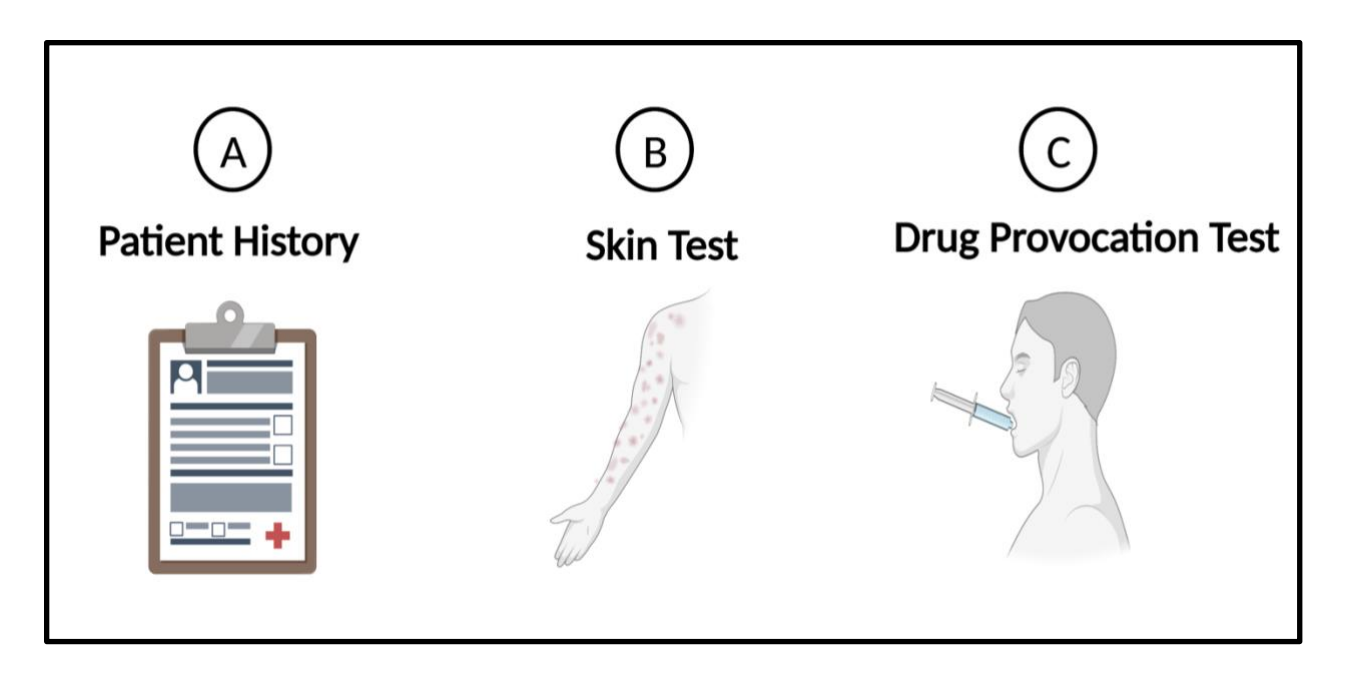


Figure 7: Diagnosing a penicillin allergy. Patients with an AAL are evaluated for their allergy using their medical history, skin tests, and/or DPTs. Patients are stratified based on their history with the drug. Lowrisk patients may be tested directly with a DPT, intermediate patients may be tested with either a DPT or a skin test, and high risk patients may require desensitization to the antibiotic before further evaluation.⁴⁶

DRUG DISCOVERY AND CLINICAL APPLICATIONS OF CHEMICAL PROBES

The advancement of small molecule inhibitors of the PD-1/PD-L1 pathway and increased insight into risk stratification of patients with a penicillin AAL can be supported through target profiling efforts; identifying and understanding the protein targets with which the small molecules inhibitors and penicillin interact with may reveal additional proteins and pathways that are implicated in the physiological responses to these molecules. This knowledge, which may be obtainable using chemical probes, can assist in structure optimization of PD-L1 inhibitors as well as the design of combination therapies aimed at targeting multiple proteins/pathways to increase treatment efficacy. Additionally, the data may identify differences between low, moderate, and high-risk patients to a penicillin allergy in a manner that improves risk stratification.

Furthermore, target profiling of the small molecule inhibitors has significant clinical implications. Chemical probes can be used against the biological fluids from patients treated with the parent drug molecule to monitor the targets of the drug at varying stages of disease and/or the targets of the drug that are associated with positive and negative responses. Such data can generate protein signatures that correlate to drug efficacy and patient response and can therefore aid in the clinical decision making behind patient treatment plans. This would be an effective and simple way to monitor disease progression and drug response throughout the course of immunotherapy in a clinically compatible way that accounts for both spatial and temporal heterogeneity of tumors.⁶⁵ In the case of drug allergy, the use of a chemical probe allows for an ex vivo detection of proteins involved in the mechanisms of an allergic response that is both safe and feasible.

RESEARCH OBJECTIVES

Target profiling of small molecules and drugs can help elucidate the endogenous targets with which they interact to generate pharmacological and physiological outcomes. The need to improve these efforts to understand and optimize small molecule immunomodulators of cancer in addition to greater understanding of the mechanisms that give rise to penicillin allergy have been established. The goal of the studies presented in this thesis is to provide a proof-of-concept to a novel chemical probe approach. This approach was employed to explore its feasibility as a target profiling method to identify binding partners of drugs that can be further investigated to assess their impact on their immunotherapeutic action or the way in which the drug elicits an allergy to penicillin.

Novel Chemical Probes Utilized in Present Study

An ABPP approach was employed in this study to synthesize chemical probes related to immunooncology and drug allergy. The warhead of each probe is derived from a parent drug compound
whose target profile is of interest, and it acts as the reactive group of the probe that interacts directly
with the protein targets. A reporter tag is used to enable target capture and is connected to the
warhead by a linker. The approach optimized in our laboratory utilizes biotin as a reporter tag and
polyethylene glycol (PEG) as a linker (Figure 8). The probes are designed for chemical probe
pulldowns in which the warhead interacts with and binds to its target proteins present in a
biological fluid. Magnetic beads coated with the immobilized bait protein, streptavidin, allow for
efficient capture and identification of target proteins using a strong magnet (Figure 8).

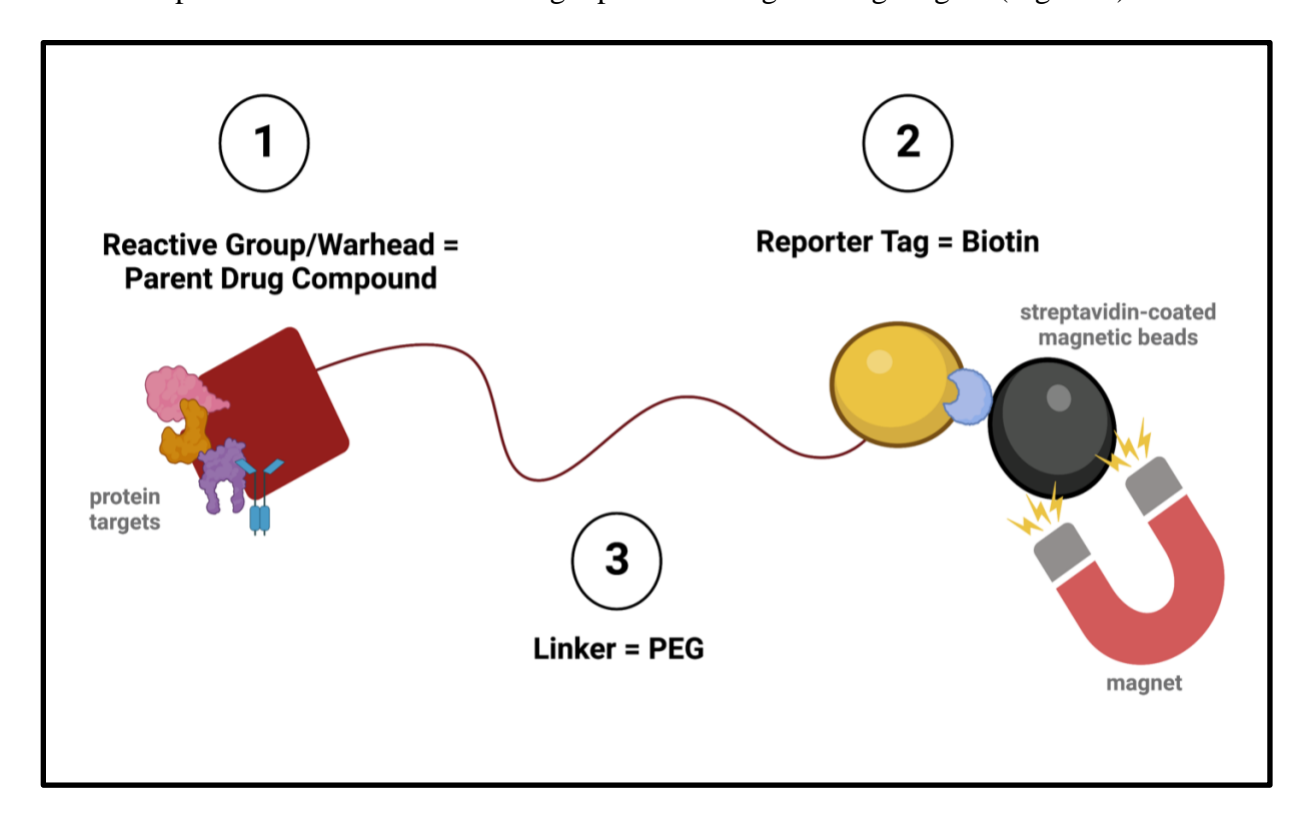


Figure 8: Illustration of chemical probe components and use. The chemical probes consist of a warhead connected to biotin via a PEG linker. The warhead interacts with its protein targets and the complex can be captured via a chemical probe pulldown using streptavidin-coated magnetic beads and a strong magnet.

The biorthogonal, complementary functional groups utilized to synthesize the probes in our lab consist of an azide, which is incorporated into the drug of interest that acts as the probe warhead, and a cyclooctyne, which is attached to the biotin-PEG moiety of the probe. The two groups undergo a strain-promoted azide-alkyne cycloaddition (SPAA) biorthogonal chemistry reaction that produces a 1,2,3-triazole group (Figure 9).

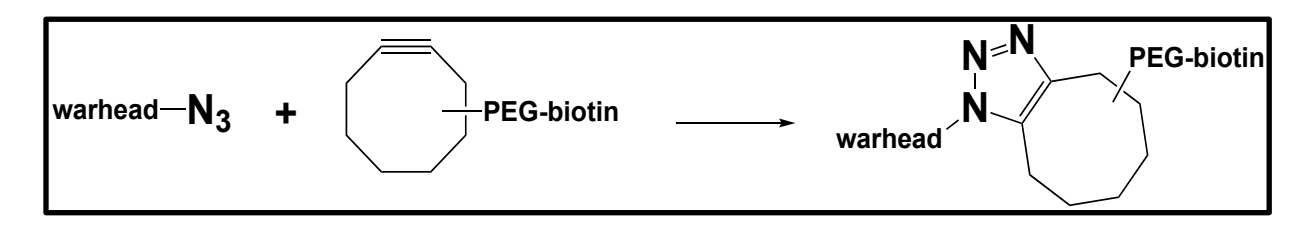


Figure 9: Strain-promoted azide-alkyne cycloaddition reaction. The SPAA reaction between a chemical probe azide warhead and cyclooctyne biotin-PEG moiety produces the 1,2,3-triazole group of the reagent probe.

The SPAA reaction can take place in situ, in which the azide warhead is introduced to the biological sample for interaction and binding to its targets prior to the addition of the cyclooctyne body for target enrichment, or in vitro, in which the reaction completes to form the reagent probe containing the 1,2,3-triazole group prior to its incubation with a sample for target fishing. Both methods were tested and will be covered in the upcoming chapters.

The experimental probe for use in the immuno-oncology portion of this study, AF147, is equipped with a warhead derived from BMS-202. The experimental probes for use in the drug allergy portion of this study carry warheads derived from ampicillin; AF132 has a warhead consisting of a closed β -lactam ring and AF239 has a warhead consisting of an open β -lactam ring. The negative control probe, AB22, has a nonspecific cyclohexane warhead that is not targeted towards any specific proteins in a biological sample (Figure 10).

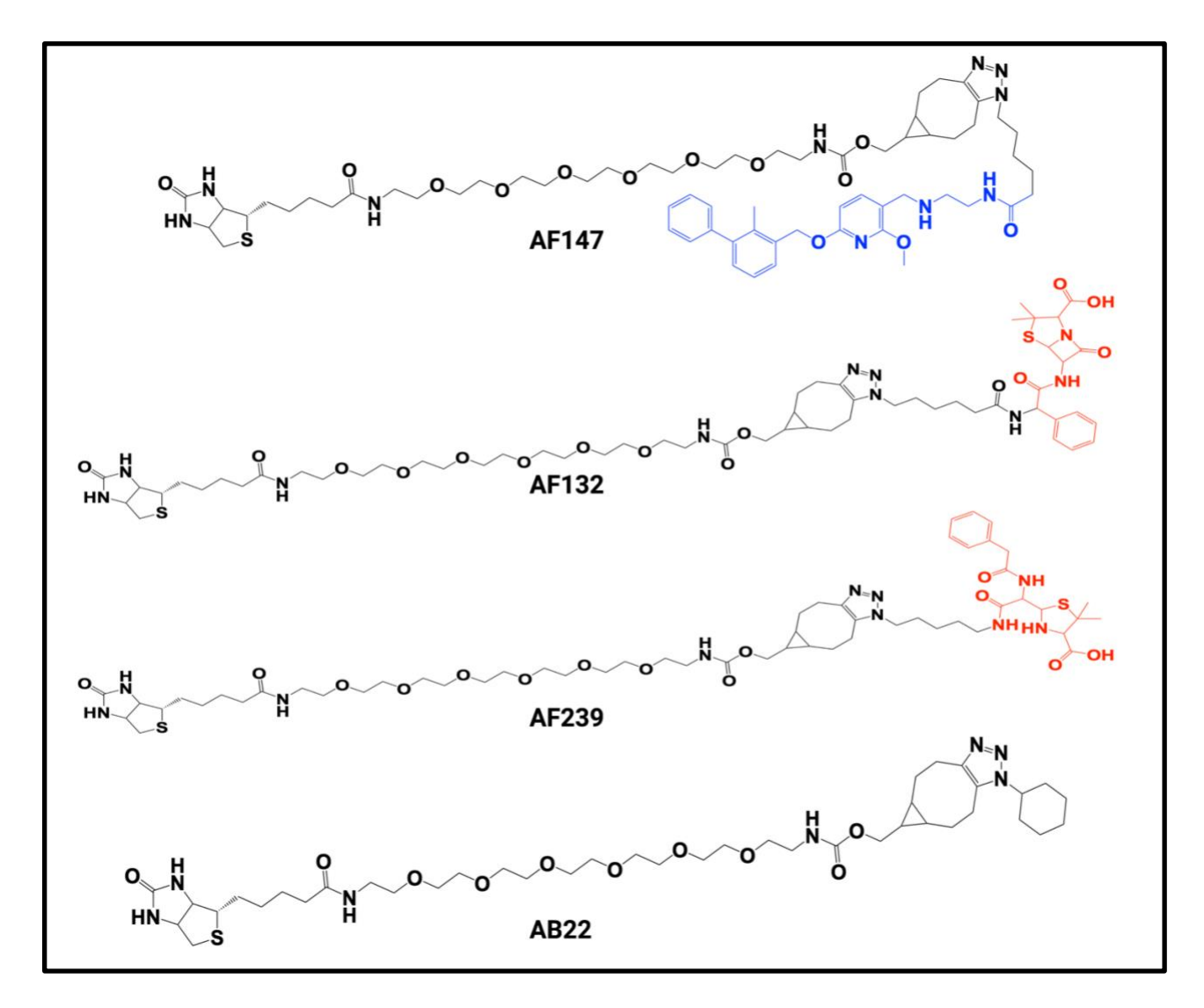


Figure 10: Chemical probes used in study. The chemical structures of AF147, AF132, AF239, and AB22. Drug scaffold is highlighted in blue (BMS-202) or red (β-lactam).

The reagent probes AF147, AF132 and AF239, in addition to their azide warhead components, AF219, AF130, and AF238, respectively, and the cyclooctyne biotin-PEG moiety, AF103, were used in various experiments for different purposes that will be explored in subsequent chapters (Figure 11).

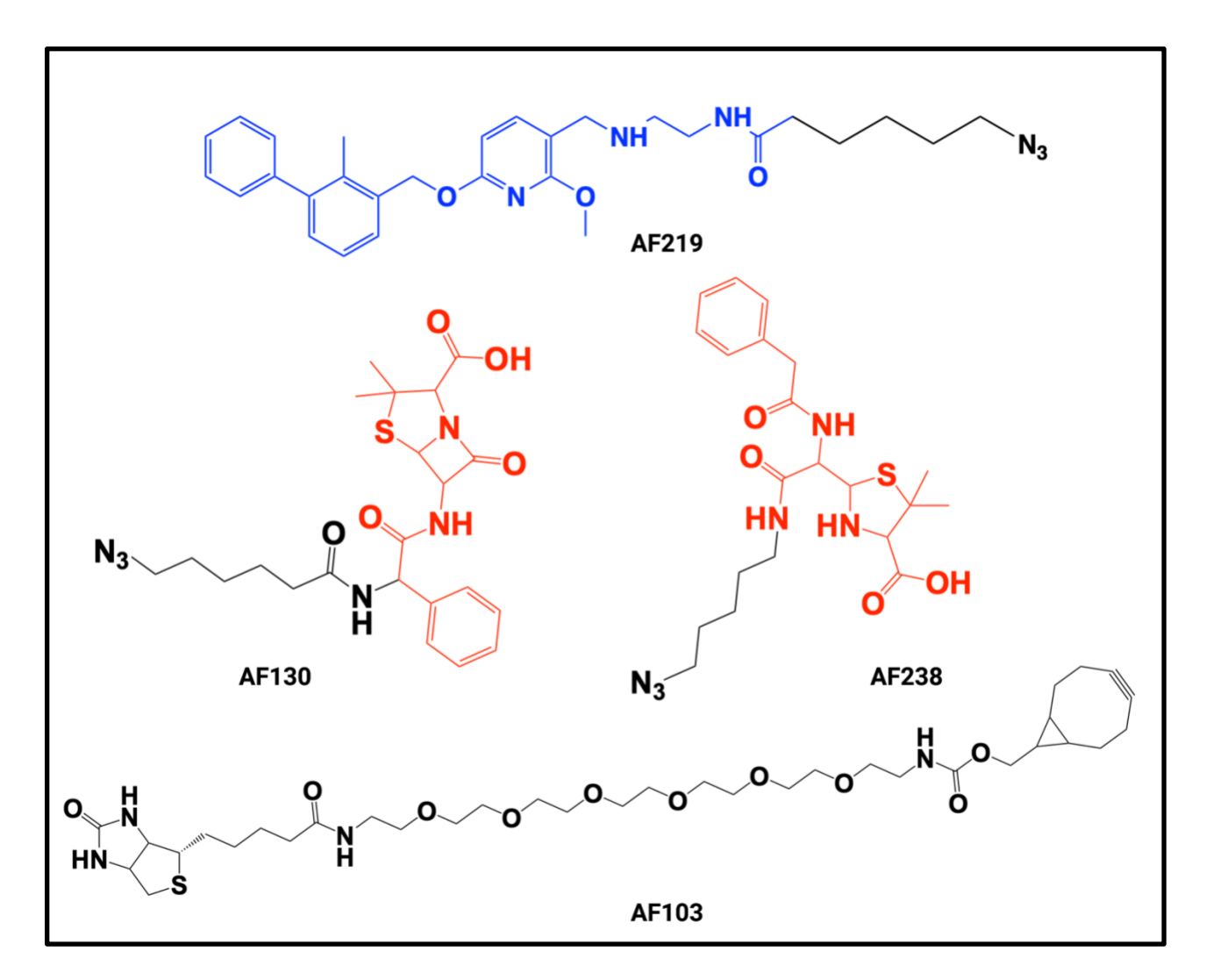


Figure 11: Biorthogonal components of probes. The chemical structures of the azide warheads AF219, AF130, and AF238. Drug scaffold is highlighted in blue (BMS-202) or red (β -lactam). The chemical structure of AF103, the cyclooctyne biotin-PEG component, is also shown.

Research Objectives

The objectives of this study are:

- To demonstrate the ability of a chemical probe tethered to a drug to identify the target binding profile of that drug.
- To use the target binding profile to rationalize potential drug combinations.

•	To explore how a chemical probe may identify molecular targets in the context of	drug
	allergy.	

CHAPTER 2

CHAPTER 2: PROFILING BIOLOGICAL SYSTEMS WITH A CHEMICAL PROBE CARRYING A SMALL MOLECULE ANTI-PD-L1 SCAFFOLD: APPLICATION TO IMMUNO-ONCOLOGY

INTRODUCTION

Combination therapies to enhance anti-cancer efficacy

Targeted immunotherapies in the form of mAbs that disrupt PD-1/PD-L1 signaling have been shown to restore antitumor activity within the TME and have led to remarkable clinical outcomes in several malignancies. However, less than 40% of patients respond to the therapies and the mechanisms underlying patient response are not fully understood. Combination therapies, in which chemo- or immunotherapeutic medications are used in tandem or alongside modalities such as surgery and ionizing radiation, have been shown to increase and prolong treatment responses among more patients. 17,24

Recent studies have highlighted synergy between chemotherapies, radiotherapies, and/or immune checkpoint blockade therapies, including anti-PD-L1 inhibition, and have identified them as possible combinations that can enhance anti-cancer activity. 66-68 Drug induced sensitization of cancer cells to another drug, or drug utilization to modulate resistance to another drug, are ways in which the combinations augment efficacious responses. Greater understanding of the mechanisms and proteins that promote cancer immunosuppression and response to certain drug/drug combinations can enhance research aimed at identifying combination therapies and patient subgroups best suited for them.

Chemical probes to identify and explore combination therapies

Chemical probes equipped with a small molecule drug scaffold as a warhead and a biotin tail designed to be captured with streptavidin-coated magnetic beads can be used as a target profiling

tool to give insight into the endogenous activity of their parental drug.^{4,9,11} The identification of drug binding partners may help predict drug response as well as reveal potential combinations to enhance activity. Such a tool can significantly advance immuno-oncology diagnostics and therapeutics.

AF147, a chemical probe with a warhead derived from BMS-202, a small molecule inhibitor of PD-L1, was employed in this study to evaluate its use as a target profiling tool (Figure 12). It was synthesized with two biorthogonal functional groups consisting of an azide warhead, AF219, and a cyclooctyne biotin-PEG body, AF103, to maintain the integrity of BMS-202 biological activity. BMS-202 is an anti-PD-L1 small molecule that physically interrupts PD-1/PD-L1 signaling by inducing PD-L1 dimerization and occluding the PD-1 binding surface. 21

Figure 12: BMS-202-equipped probe. Structure of AF147 and AF219. BMS-202 scaffold is highlighted in blue.

Initial studies using AF147 and AF219 were completed to ensure that they maintained the activity of BMS-202. Chemical probe pulldowns with AF147 were then completed on cancer cell lysates to develop a binding signature for BMS-202 using proteomic mass spectroscopy. We identified DNA-PKcs, a component of DNA-PK, as a prominent binding partner of BMS-202 and challenged its function by comparing its growth inhibitory profile with that of NU7026, a specific inhibitor of DNA-PK. Previous studies have shown that NU7026 sensitizes cells to doxorubicin, an antitumor antibiotic that induces DSBs in human tumor cells, which are known to be repaired by DNA-PK. 43,69,70 We assume that if DNA-PKcs is indeed a target of BMS-202 it should similarly potentiate doxorubicin. Thus, we have compared the ability of BMS-202 to synergize with doxorubicin to that of NU7026. Growth inhibition assays with NU7026 and BMS-202 revealed that the two inhibitors both synergize with doxorubicin to exert antiproliferative activity against two cancer cell lines.

In addition to the analysis of BMS-202 synergy with doxorubic to elucidate its potential function as a DNA-PK inhibitor, we also analyzed the effect of multiple dose exposure to BMS-202 on its target binding profile. AF147 was able to detect a change in the BMS-202 binding signature following prolonged drug exposure. Here we describe the potential DNA-PK inhibitory function of BMS-202 and probed target modification that it induced following multiple dose exposure.

METHODS AND MATERIALS

Chemical Probe Preparation/Drug Treatment

All probes (AF147, AF219, AF103, and AB22), as well as BMS-202, were synthesized in our laboratory. Doxorubicin and NU7026 were purchased from the McGill University Health Centre

pharmacy (Montréal, QC, CA) and MedChem Express (Monmouth Junction, NJ, USA), respectively. Olaparib (MedChem Express) was generously given by the laboratory of Dr. Jean-Jacques Lebrun. Stock solutions (10-25mM) of all molecules were prepared in DMSO under sterile conditions. All stock solutions were diluted in different solvents to various concentrations in accordance with the specific protocol they were being prepared for.

Homogenous Time Resolved Fluorescence (HTRF) PD-1/PD-L1 Binding Assay

The HTRF PD1: PD-L1 Binding Assay (Perkin Elmer, Waltham, MA, USA) was completed to determine the IC₅₀ values of AF147 towards PD-1: PD-L1 binding. The interaction of PD-1 with PD-L1 triggers fluorescence resonance energy transfer, or FRET, between an HTRF donor, Europium labeled anti-Tag1, and an HTRF acceptor, XL665 labeled anti-Tag2. The signal corresponds to the level of interaction between the two proteins and is therefore reduced by the addition of inhibitory compounds.

Signal measurements were collected using 6-fold serial dilutions with a maximum concentration of $100\mu\text{M}$ for AF147. All components of the assay were mixed to reach the final $20\mu\text{L}$ volume in accordance with the protocol and then incubated for one hour before measuring the HTRF signal. A Tecan Infinite 200Pro plate reader was used to determine the optical density (OD) of each well at 665nm and 620nm. The HTRF ratio was calculated using the formula: $HTRF\ Ratio = \frac{oD_{665nm}}{oD_{620nm}} \times 10^4$. Analysis of the IC₅₀ values was completed using GraphPad Prism 9.4.1 (GraphPadSoftware, Inc., San Diego, CA, USA).

Cell Culture

The human osteosarcoma cell line (SAOS-2; ATCC: HTB-85) and mouse fibroblast cell line (NIH WT; ATCC: CRL-1658) were maintained in RPMI medium. The human lung carcinoma cell line (A549 WT; ATCC: CRM-CCL-185), as well as two cell lines derived from Chinese hamster lung cancer cells, V-C8 WT and V-C8 BRCA, were maintained in DMEM medium. Both RPMI and DMEM mediums were supplemented with 10% (v/v) fetal bovine serum. The cells were kept in incubators that maintained 5% CO₂ at 37°C. All cells used in this study were thawed from frozen aliquots of previously purchased or gifted cell lines. All cells were subcultured, or passaged, under sterile conditions when their confluency reached about 80% within their respective flasks.

1. SAOS-2 Multiple Dose Exposure to BMS-202

A population of SAOS-2 cells (P₀) was exposed to 0.1μM BMS-202 over 10 passages (P₁₀) to evaluate the resulting PD-L1 levels, BMS-202 IC₅₀, and BMS-202 binding partner signature.

2. SAOS-2 AF219 Treatment

Another population of SAOS-2 cells was treated with $5\mu M$ AF219 for 15, 30, 60, 180, and 360min to evaluate the effect on PD-L1 levels.

Magnetic Bead Pulldown with Chemical Probe

Solutions of 10µM AF147 or AF219 were prepared and pre-immobilized onto streptavidin magnetic beads (ThermoFisher Scientific, Waltham, MA, USA) prior to their incubation with 50µL of cell lysate. In some experiments, different amounts of an exogenous, human recombinant PD-L1 (Abcam, Cambridge, UK) were added to the cell lysates or control serum. The mixture was agitated with a tube rotator during the incubation period to facilitate the binding of PD-L1 to the anti-PD-L1 moiety of the probe. The beads were then cleared of excess cell lysate and washed.

For western blot analysis, 2x Laemmli Sample Buffer (BioRad, Hercules, CA, USA) was used at this stage to elute the captured proteins from the beads. For proteomic analysis, an overnight, on-bead digestion of the immunoprecipitated proteins was carried out using 12ng/µL trypsin (Promega, Madison, WI, USA) at 37°C. Digestion was stopped and the peptides were eluted from the beads using HPLC grade acetonitrile (Fischer Scientific, Waltham, MA, USA). The solution containing the peptides was collected and subsequently dried using a SpeedVac Vacuum Concentrator. Lastly, the peptides were identified using proteomic mass spectrometry. An illustration of this process is displayed in Figure 13.

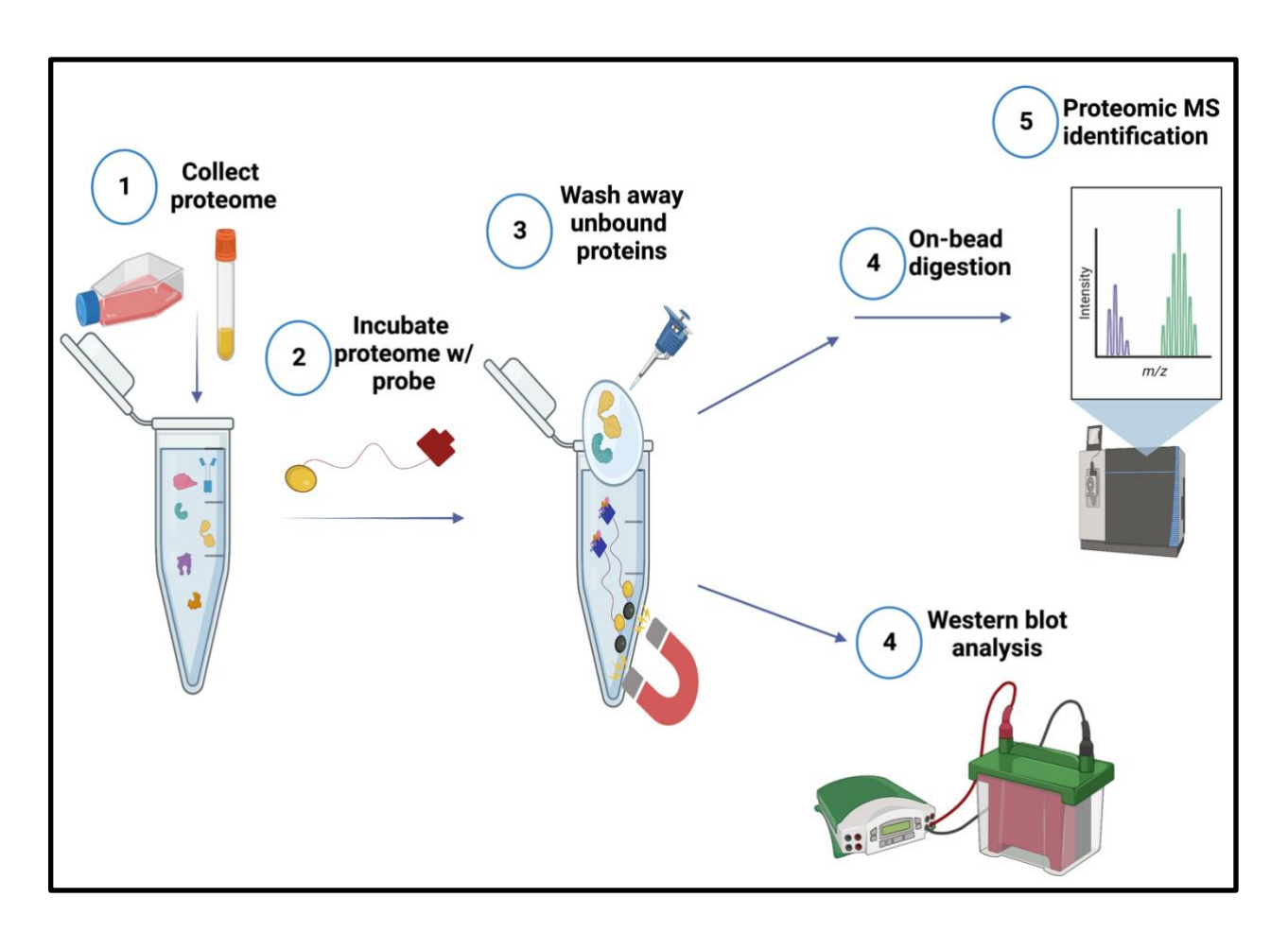


Figure 13: Illustration of chemical probe pulldown. The proteome of cell lysates or serum is collected and then incubated with the chemical probe. A magnet is used to retain the captured protein-chemical probe

complexes as the rest of the sample is discarded. Captured proteins are identified via proteomic mass spectrometry or western blot.

Western Blot

SAOS-2 (untreated, BMS-202 multiple dose exposed, and AF219 treated), NIH WT, and A549 WT cells were plated (~0.5 x 10⁶ cells/well) in 6-well plates to adhere overnight in an incubator maintained at 5% CO₂ and 37°C. After 24hrs, the cells were washed twice with PBS and detached through scraping and a 10-minute incubation at 4°C with 1X RIPA lysis and extraction buffer (ThermoFisher) supplemented with 0.1% of a protease inhibitor, phenylmethylsulfonyl fluoride (Sigma, St. Louis, MO, USA). Lysates were collected by centrifugation at 15000rpm for 15min at 4°C. The protein concentrations of the lysates were determined using a Bradford assay completed with a BSA protein standard and a Protein Assay Dye Reagent Concentrate (Bio-Rad).

A total of 30µg of protein, or all of the proteins captured from pulldowns against serum, were loaded and resolved on 10% SDS-PAGE and then transferred to to a polyvinylidenedifluoride (PVDF) membrane (Bio-Rad). Membranes were blocked with 5% BSA in 0.1% PBST for 45min at room temperature prior to an overnight incubation at 4°C with an anti-PD-L1 antibody (New England Biolabs, Ipswich, MA, USA) diluted 1:1000 in 5% BSA in 0.1% PBST. The membranes were then washed three times with 0.2% PBST and incubated for one hour at room temperature with an anti-rabbit secondary antibody (Abcam) diluted 1:8000 in 1% BSA in 0.2% PBST. After three more washes with 0.2% PBST, the presence or absence of PD-L1 was determined using PierceTM ECL Western Blotting Substrate (ThermoFisher).

Proteomic Mass Spectrometry

1. Liquid Chromatography Tandem Mass Spectrometry (LC-MS-MS)

An EASY-nLC 1000 Ultra-High-Performance Liquid Chromatography (UHPLC) system (Thermo Scientific, Waltham, MA, USA) was coupled with a Q Exactive HF hybrid quadrupole-Orbitrap mass spectrometer (Thermo Scientific) for the proteomic liquid chromatography—mass spectrometry (LC—MS) analysis. A C18 column (Acclaim C18 Column, Thermo Scientific) fitted with a trapping column (Acclaim PepMap100, Thermo Scientific) was used to separate rehydrated tryptic peptide fragments; a 100min 3-38% buffer B gradient (99.9% acetonitrile, 0.1% formic acid) was used to elute the peptides over a total run time of 120min at a flow rate of 350nL/min. The MS was operated in data-dependent mode and acquired survey scans with a 375-1400m/z range, 120 000 resolution at m/z=200, an AGC target of 5E6, and a maximal ion injection time of 60ms. The 25 most abundant isotopes detected with a change ≥ 2m/z were subjected to fragmentation by higher energy collisional dissociation at a normalized collision energy of 25 eV. The MS/MS was performed with 15000 resolution, an ion isolation window of 2.5m/z, an AGC target of 2E5, and a maximal ion injection time of 60ms. A 3.5s dynamic exclusion time was used. Data acquisition was completed with Xcalibur Software (Thermo Scientific).

2. Bioinformatics Analysis

Processing of the MS data files was completed using the Mascot Distiller interface (Matrix Science Ltd, London, UK). The Mascot search engine identified peptides and proteins from the MS files with a significance threshold of 0.05 ($p \le 0.05$). The results were imported to Scaffold (Proteome Software, Portland, OR, USA) for additional analysis at a false discovery rate (FDR) of < 5%.

Growth Inhibition Assay

The sulforhodamine B (SRB) assay was the specific growth inhibition assay employed in this study for cytotoxicity screening of drug compounds. SAOS-2, V-C8 WT, and V-C8 BRCA cells were plated in 96-well plates (Corning, Corning, NY, USA) with a volume of 100µL at concentrations of 3000, 2500, and 1500cells/well, respectively. Wells along the perimeter of the plates were loaded with 200µL of PBS to minimize volume changes that could affect cells due to evaporation. The cells were treated after a 24hr incubation at 5% CO₂ and 37°C in which the cells adhered to the plate. The treatments used against the cells are described in Table 1.

Table 1: Experimental design of growth inhibition assays to compare the effects of BMS-202 and NU7026 on the potency of doxorubicin in cancer cells.

Objective	Cell Line	Drug	Concentration (uM)
Assessment of drug IC ₅₀	Untreated SAOS-2	BMS202	0-50
		NU7026	0-200
	V-C8, V-C8 BRCA	Olaparib	0-10 (V-C8) 0-75 (V-C8 BRCA)
		BMS-202	0-50
		NU7026	0-200
		Doxorubicin	0-10
	BMS-202 exposed SAOS-2 cells	BMS202	0-75
Assessment of drug PI ₅₀	Untreated SAOS-2, V-C8, V-C8 BRCA	BMS-202 w/ NU7026	0-50 BMS 10 NU7026
Synergy determination and CI ₅₀	V-C8	Doxorubicin and NU7026	0-1 Doxorubicn 0-100 NU7026
		Doxorubicin and BMS- 202	0-0.64 Doxorubicin 0-21.3 BMS-202
	V-C8 BRCA	Doxorubicin and NU7026	0-2 Doxorubicn 0-100 NU7026
		Doxorubicin and BMS- 202	0-0.75 Doxorubicin 0-12.5 BMS-202

Following a 5-day incubation period, the cells were exposed to 50µL of 50% trichloroacetic acid (ThermoFisher) for 2 hours at 4°C for fixation. The cells were washed three times with water

and left to dry overnight before being stained with 100µL/well of a 0.4% SRB solution (ThermoFisher) for two hours. The excess SRB dye was removed with three washes of 1% (v/v) acetic acid (ThermoFisher). After a second overnight drying period, the protein-bound dye was dissolved using 200µL/well of a 10mM Tris base solution (ThermoFisher). A Tecan Infinite 200Pro plate reader was used to determine the OD of each well at 520nm. Each experiment was completed in triplicates and replicated at least two times.

Calculation of the IC₅₀ values was completed using GraphPad Prism 9.4.1 (GraphPadSoftware, Inc., San Diego, CA, USA). Potentiation factors at 50% growth inhibition (PF₅₀) were determined from the ratio of the IC₅₀ of BMS-202 alone divided by the IC₅₀ of BMS-202 when used with 10µM of NU7026.⁷¹

The calculation of the combination index (CI) to evaluate synergy between drugs was completed using the Chou-Talalay method.⁷² The ratio of concentrations used for the two drugs, drugs A and B, was derived from the ratio of their individual IC₅₀ values (labeled as γ A and γ B) and maintained at each dilution. The CI₅₀ was calculated using the IC₅₀ of each drug individually with the IC₅₀ of each drug when used in combination (γ c) using the formula: $CI_{50} = \frac{\gamma A_C}{\gamma_A} + \frac{\gamma B_C}{\gamma_B}$.⁷² Additional CI values were calculated to construct isobolograms for graphical representations of the interactions between the drugs. They were calculated using the same formula as the CI₅₀ but with inhibitory concentration values ranging from 10-90% inhibition. These values were calculated from the drug combination growth inhibition curves using the formula: $Y = Bottom + \frac{(Top-Bottom)}{1+10!(ICS0-x)\times Hill Slope}$, where bottom refers to the basal cell viability, top refers to the maximal cell viability, and the hill slope refers to the steepness of the growth inhibition curve. CI values >1, =1, and <1 correspond to antagonistic, additive, and synergistic interactions between the two drugs, respectively.⁷²

Statistical Analysis

Statistical analysis was performed using GraphPad Prism 9.4.1. Significance was found when data from two or more independent experiments was available using the unpaired, two-tailed student t-test. Statistical significance was determined from p values <0.05. Data shown represent mean \pm SD.

RESULTS

AF147 inhibits PD-1/PD-L1 binding more strongly than BMS-202

The IC₅₀ of AF147 towards PD-1: PD-L1 binding was calculated using the HTRF PD1: PD-L1 Binding Assay. AF147 was found to be inhibitory with an IC₅₀ value of $0.017\mu M$ (Figure 14). AF147 demonstrated PD-1/PD-L1 inhibition similar to BMS-202 based on its reported HTRF IC₅₀ value of $0.018 \,\mu M.^{21}$

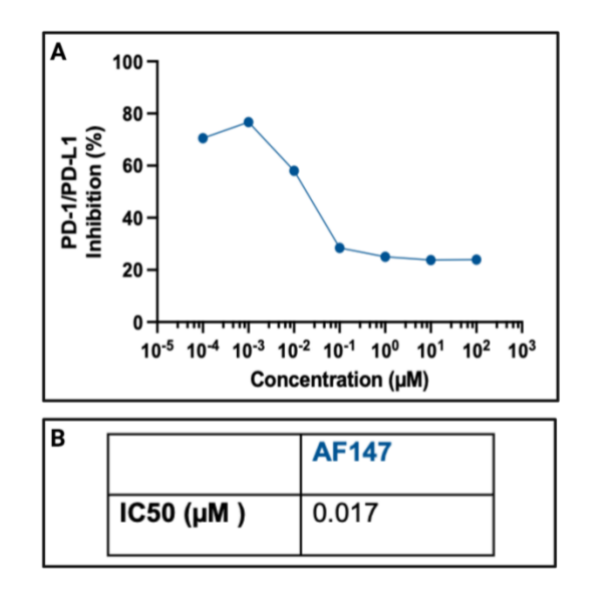


Figure 14: Inhibition of PD-1/PD-L1 binding by AF147. (A) PD-1/PD-L1 inhibition curve generated by an HTRF binding assay using AF147. (B) Corresponding IC₅₀ value for AF147.

AF147 does not capture PD-L1 from cell lysates or serum

Although AF147 was shown to be effective at targeting PD-L1 from the HTRF assay, it did not capture PD-L1 from the cell lysates of SAOS-2, NIH WT, or A549 WT cells. Western blot detection of PD-L1 was completed on cell lysates before and after a chemical probe pulldown with AF147. PD-L1 was detected before the pulldown but not after it (Figure 15A). β -actin was detected both before and after the pulldown.

Exogenous PD-L1 was added to NIH WT cell lysates to assess if an increase in PD-L1 concentration would assist in its capture by AF147. A range of PD-L1 concentrations from 0 to 8ng was used to determine if there was a threshold concentration needed for its capture. PD-L1 was detected in the lysates before a chemical probe pulldown with AF147 but its signal was lost after the pulldown (Figure 15B). The added PD-L1, which should migrate to 30-35kD according to its manufacturer, was not detected even before a pulldown. β-actin was detected in the lysates both before and after the pulldown.

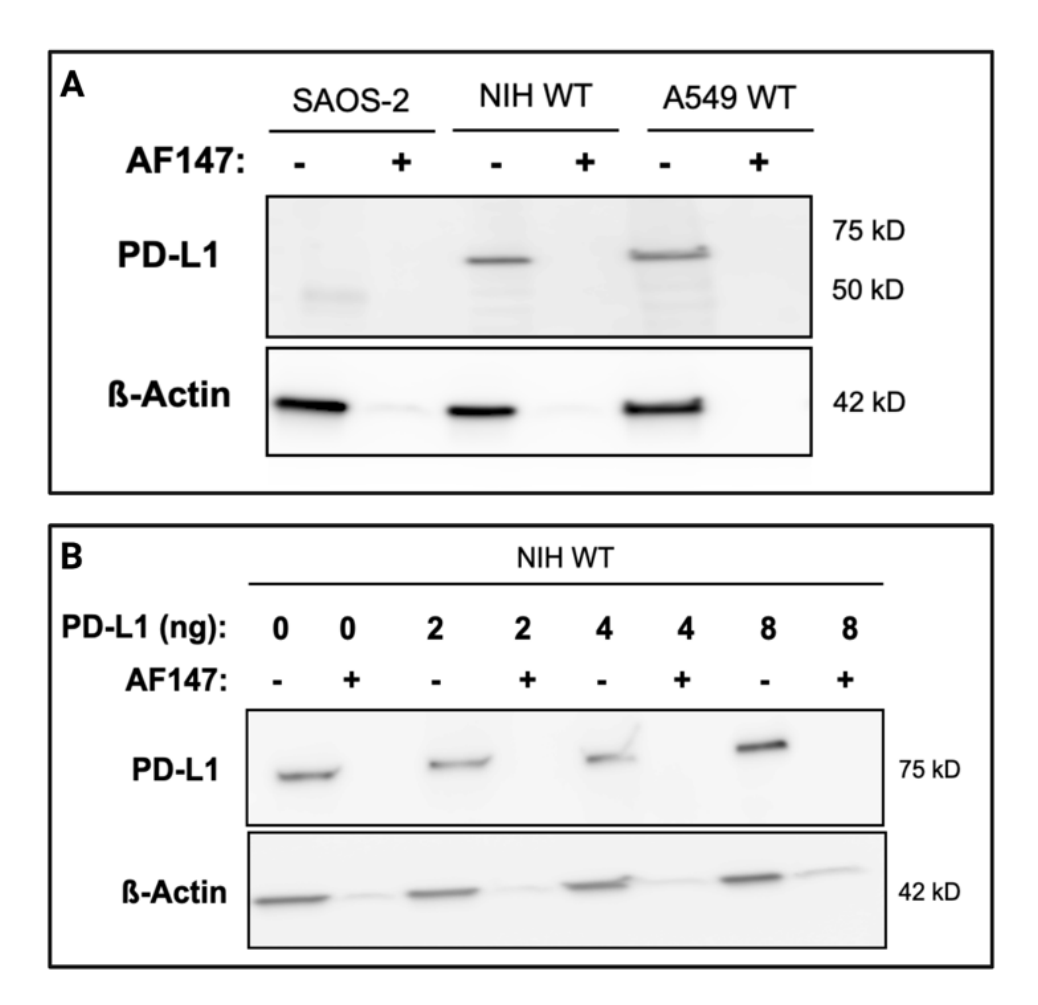


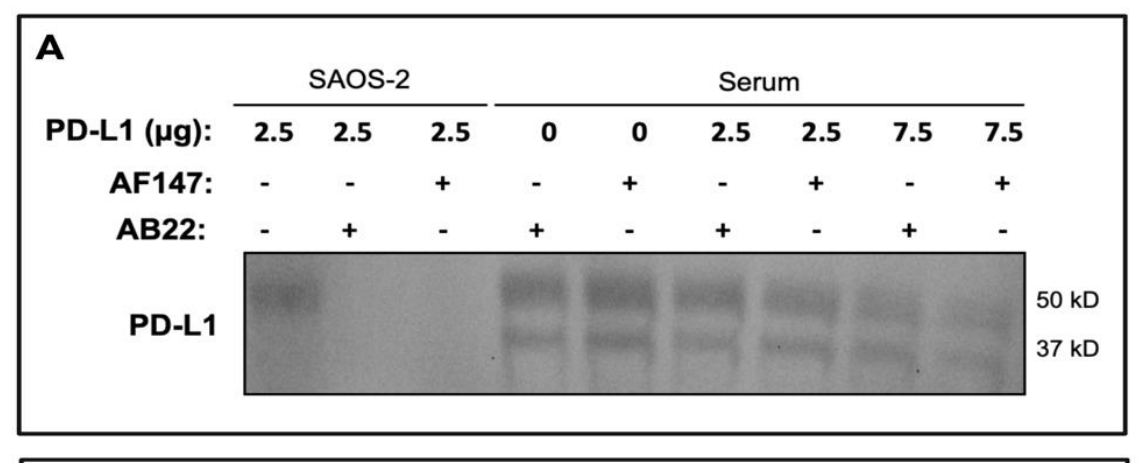
Figure 15: PD-L1 detection in cell lysates via western blot analysis. (A) The cell lysates of SAOS-2, NIH WT, or A549 WT cells were analyzed before (-) and after (+) a chemical probe pulldown with AF147 to detect the presence of PD-L1 in samples. PD-L1 was detected before the pulldowns but not after them.

(B) Exogenous PD-L1 (0, 2, 4, and 8ng) was added to cell lysates of NIH WT cells to determine if an increase in PD-L1 concentration would assist in its capture by AF147. PD-L1 was detected before (-) the pulldowns but not after (+) them.

Another chemical probe pulldown was completed in which 2.5 and 7.5µg of exogenous PD-L1 was added to human serum. This was done to assess whether AF147 was able to capture its primary target from a serum milieu, the biological sample that the chemical probe will ultimately be used against in clinical settings. As seen in Figure 16A, a signal was detected at 50kD

from the serum samples, however this seems to correlate to denatured IgG present in serum that was captured by both AF147 and the negative control probe, AB22. The serum samples also show a signal at 37kD, but this is also attributed to the secondary antibody detection of denatured IgG present in the serum rather than to the added PD-L1. This conclusion is supported by the presence of the same signal in the 0µg PD-L1 serum sample and its absence in the SAOS-2 cell lysates, which were used to evaluate the serum results more thoroughly.

Finally, a pulldown was completed with the biorthogonal, complementary functional parts of AF147 to determine whether the biological activity of its BMS-202 warhead was affected by the biotin-PEG moiety of the probe; AF219, its azide warhead component, was used against human serum with 5ng of added PD-L1 before the SPAA reaction of AF219 with AF103, the cyclooctyne biotin-PEG moiety. As shown in Figure 16B, the presumed 50kD heavy chain of IgG was once again detected. The 50kD portion of the membrane was removed to avoid interference from the heavy chain of endogenous IgG and the possibility that it masked a weaker PD-L1 signal. The membrane was visualized again, and the added PD-L1 was not detected. AF147, as well as AF219 and AF103, were incapable of capturing PD-L1.



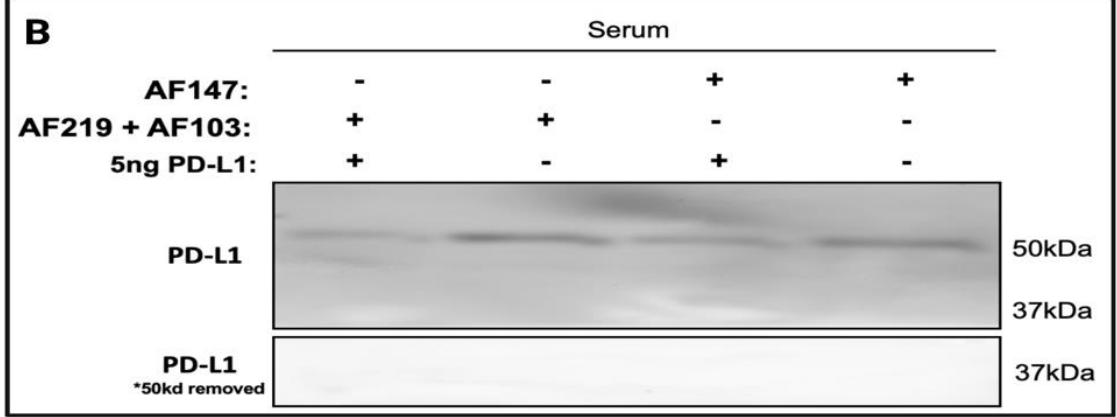


Figure 16: PD-L1 detection in serum via western blot analysis. (A) Exogenous PD-L1 (0, 2.5, and 7.5μg) was added to human serum to determine if a different biological sample would enable AF147 to capture its primary target. SAOS-2 cell lysates were used for comparison. PD-L1 was not detected after an AF147 pulldown. (B) The biorthogonal, complementary functional parts of AF147, AF219 and AF103, were used against serum with 5ng of added PD-L1 to determine whether the biological activity of its BMS-202 warhead was compromised by the biotin-PEG moiety of the probe. PD-L1 was not detected in the pulldown by AF219 and AF103 or by AF147.

AF219 increases SAOS-2 PD-L1 levels over a 6-hour treatment

To further assess the extent of the probe activity with PD-L1, SAOS-2 cells were treated with 5μM of AF219. AF219 was used for this experiment since a pulldown was not the objective, and therefore the biotin-PEG body was not needed for target capture. The relative PD-L1 expression

levels were quantified via western blot after 15, 30, 60, 180, and 360 min using the untreated cells as the reference sample and ß-actin as the loading control. The relative PD-L1 levels gradually increased over the course of the AF219 treatment, with the greatest increase seen between 60 and 180min, in which the expression doubles (Figure 17). Interestingly, it has been shown that cell exposure to anti-PD-L1 inhibitors leads to a transient increase in PD-L1 levels.⁷³ When SAOS-2 cells were exposed to AF219, the relative PD-L1 levels increased consistently over the 6-hour treatment.

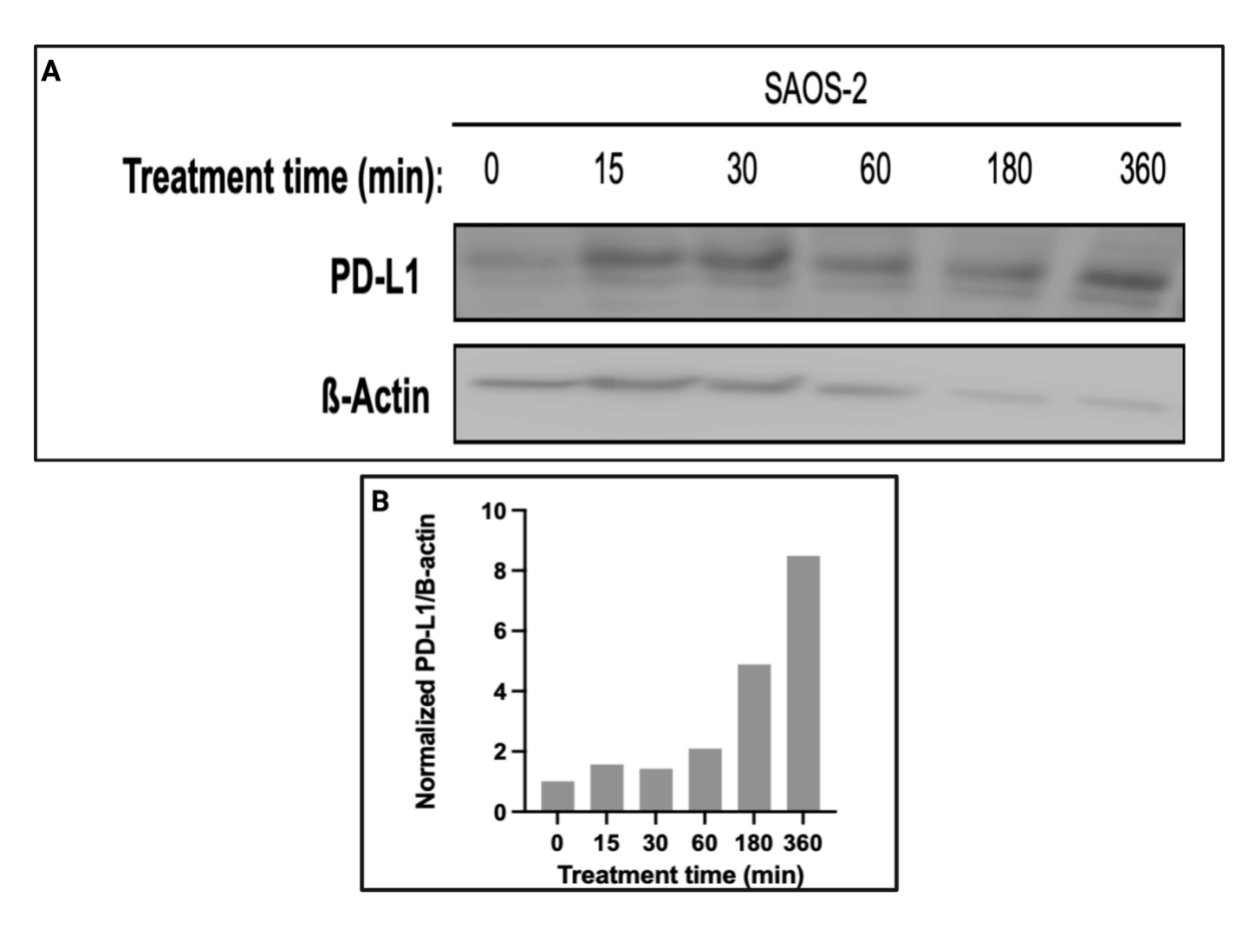


Figure 17: AF219 treatment increases relative PD-L1 levels in SAOS-2 cells. (A) SAOS-2 cell lysates were analyzed via western blot analysis for their relative levels of PD-L1 following 0, 15, 30, 60, 180 or 360min treatment times with AF219. (B) The corresponding graphical representation of relative PD-L1 levels from the various treatment times with AF219.

AF147 captures cell lysate proteins implicated in malignancies

Chemical probe pulldowns of AF147 against SAOS-2 and A549 WT cell lysates were completed to identify the secondary targets of the BMS-202 warhead using proteomic mass spectroscopy. The proteins captured by the experimental probe were identified using AB22, the negative control probe, which lacks an active warhead. The targets of the BMS-202 warhead were identified as proteins that were captured by AF147 but not by AB22. The most prominent and relevant proteins detected from each cell line are displayed in Table 2. All proteins have been implicated in different types of malignancies, which suggests that AF147 can capture proteins involved in the biological processes targeted by its warhead.

Table 2: BMS-202 binding partners in SAOS-2 and A549 WT cells identified using proteomic mass spectrometry.

Α	SAOS-2: BMS-202 Binding Partners	Total Spectrum Count
	Tubulin alpha-1B chain	+++
	DNA-PKcs	+++
	Cullin-associated NEDD8-dissociated protein 1	++
	Exportin-2	+
	Extracellular hemoglobin	+
	Importin-7	+
	Exportin-5	+
	Mic60/mitofilin	+
	Translational activator GCN1	+
	Importin-5	+
	Exportin-1	+
Spect	rum counts: high range (+++) = 20+, mid-range (++) =	= 10-20, low-range (+) = 3-10
В	A549 WT: BMS-202 Binding Partners	Total Spectrum Count
	DNA-PKcs	+++
	Translational activator GCN1	+++
	Mic60/mitofilin	+++
	Exportin-1	++
	Tubulin alpha-1B chain	++
	78-kDa glucose-regulated protein	++
	Peroxiredoxin-1	++

Spectrum counts: high range (+++) = 50+, mid-range (++) = 25-50, low-range (+) = 10-25

Exportin-2

Importin-7
Importin-5

(A) BMS-202 binding partners identified in SAOS-2 cells. (B) BMS-202 binding partners identified in A549 WT cells. The binding partners displayed were determined from the Scaffold generated data on the captured proteins detected from chemical probe pulldowns. Total spectrum counts refer to the total number of spectra identified for a protein from each sample of captured proteins. The proteomics software identified proteins with FDR < 5% and p < 0.05. Binding partners of BMS-202 were identified as proteins that were captured by AF147 but not by AB22.

+

NU7026 does not potentiate BMS-202 activity

DNA dependent protein kinase catalytic subunit (DNA PK-cs) was identified as a prominent binding partner of the AF147 BMS-202 warhead in both SAOS-2 and A549 WT cells. DNA-PKcs is a component of DNA-PK.⁴⁰ To assess the impact of DNA PK-cs on BMS-202 activity, a specific inhibitor of DNA-PK, NU7026 (2-(morpholin-4-yl)-benzo[h]chomen-4-one), was used in a series of growth inhibition assays.⁷¹ It was first used to determine if DNA-PK inhibition potentiated BMS-202 cytotoxicity on SAOS-2, V-C8, and V-C8 BRCA cells.

The SAOS-2 cell line was used for this experiment as it was one cell line in which DNA-PKcs was identified as a binding partner of BMS-202. V-C8 WT cells, which are defective in BRCA2 and are therefore HR deficient, as well as their corresponding BRCA transfectant, V-C8 BRCA, were used to identify synthetically lethal interactions between PD-L1 and BRCA2, or between DNA-PK and BRCA2, as illustrated by the selective potency of BMS-202 or NU7026, respectively, on the growth inhibition of the WT mutant cells.⁷⁴ To ensure the integrity of the BRCA transfectant, the selectivity of olaparib, a PARP1 inhibitor, towards the WT mutant was tested and confirmed through it significant potency seen in the V-C8 WT cells (Figure 18).

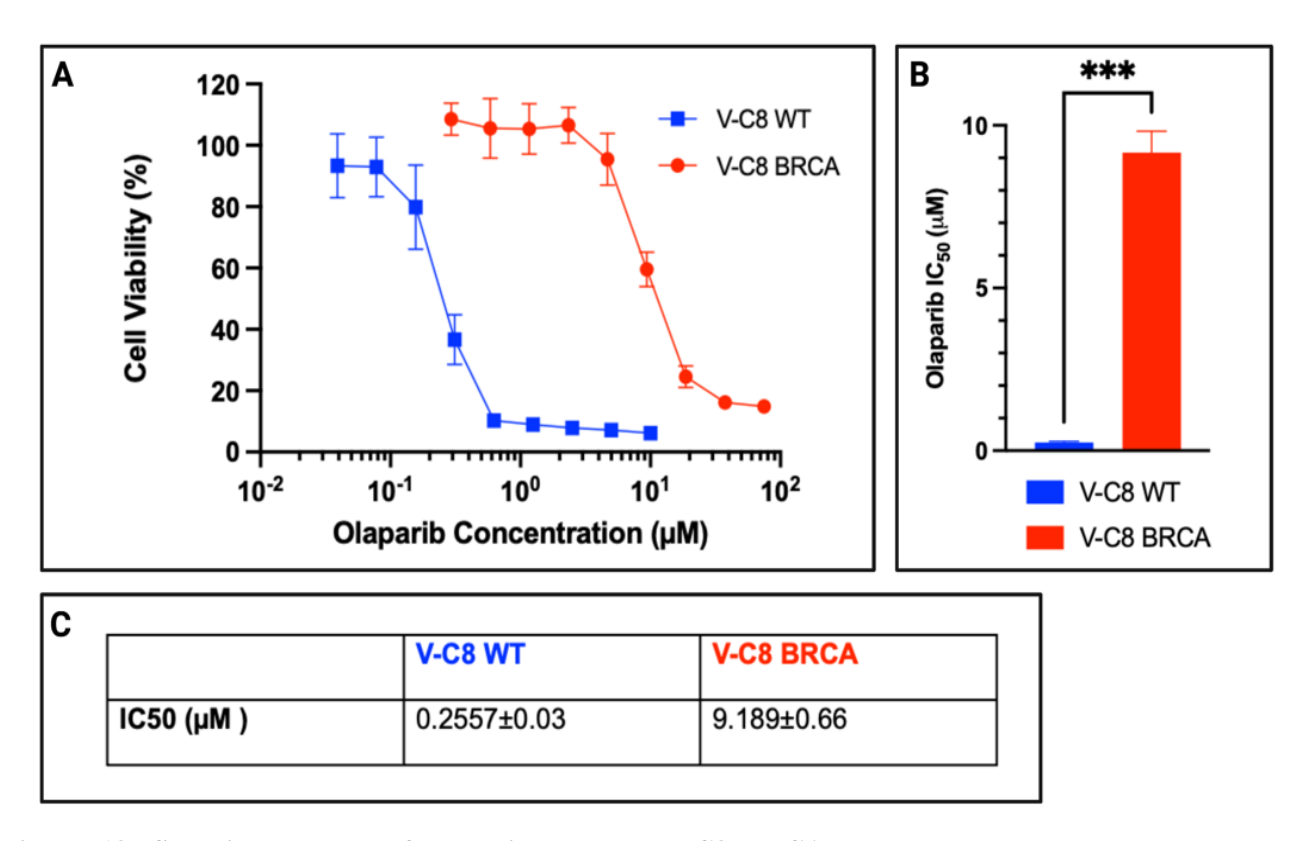
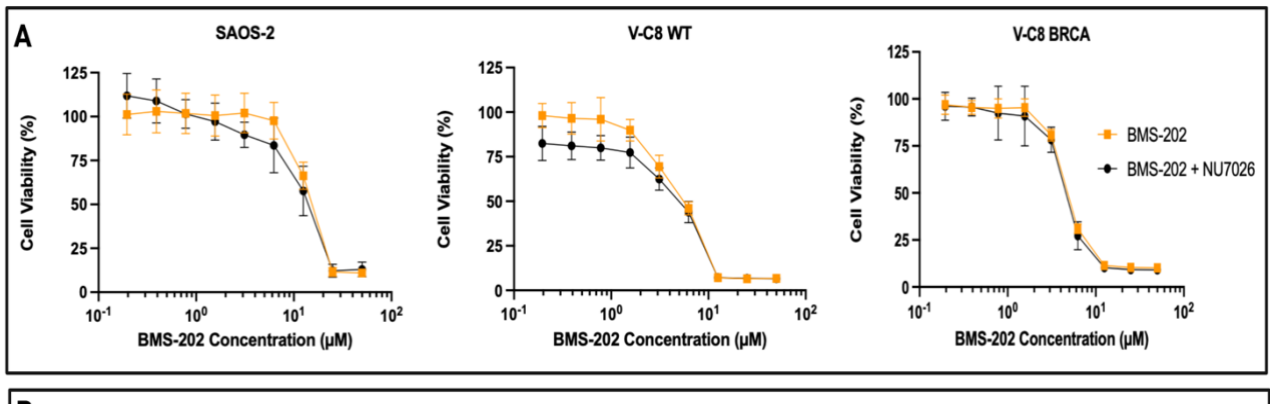


Figure 18: Selective potency of olaparib towards V-C8 BRCA cells. (A) Comparison of growth inhibition curves of Olaparib in V-C8 WT and V-C8 BRCA cells. (B) Comparison of the corresponding IC₅₀ values for V-C8 WT and V-C8 BRCA cells. (C) Olaparib IC₅₀ values in each cell line.

Figure 19A displays the concentration-dependent effects of BMS-202 alone and BMS-202 in the presence of a fixed concentration of 10μM NU7026 on the three cell lines. The corresponding IC₅₀ values, along with that of NU7026 for each cell line, as well as the PF₅₀ value of NU7026 on BMS-202, are listed in Figure 19B. NU7026 minimally potentiated the growth inhibitory effects of BMS-202 in SAOS-2 cells (PF=1.21), did not demonstrate potentiation in V-C8 BRCA cells (PF=1.03), and contrarily, appeared to offer minimal protection to V-C8 WT cells from BMS-202 (PF=0.84). Neither BMS-202 nor NU7026 displayed any selectivity for the WT mutant cells as demonstrated by their IC₅₀ values, thus indicating that PD-L1 and DNA-PK do not have synthetically lethal interactions with BRCA2.



	NU7026 (μM)	BMS-202 (µM)	BMS-202 + 10uM NU7036 (μM)	PF_{50}
SAOS-2	23.28 ± 0.08	13.56 ± 0.04	11.24 ± 0.46	1.21
V-C8 WT	14.59 ± 0.69	5.022 ± 0.08 uM	5.969 ± 0.28	0.84
V-C8 BRCA	11.83 ± 1.3	4.662 ± 0.02	4.505 ± 0.40	1.03

Figure 19: NU7026 did not show potentiation of BMS-202 growth inhibition. (A) Comparison of growth inhibition curves of BMS-202 alone and BMS-202 in the presence of 10μM NU7026 in SAOS-2, V-C8 WT, and V-C8 BRCA cells. (B) Corresponding IC₅₀ and PF₅₀ values in each cell line.

BMS-202 and NU7026 interact synergistically with Doxorubicin

To further investigate DNA-PKcs as a binding partner of BMS-202, a series of growth inhibition assays were conducted to determine if BMS-202 and NU7026 synergize with doxorubicin. The growth inhibition data from the individual drugs (Figure 20) was used to determine the equieffective combinations needed to test synergy.⁷²

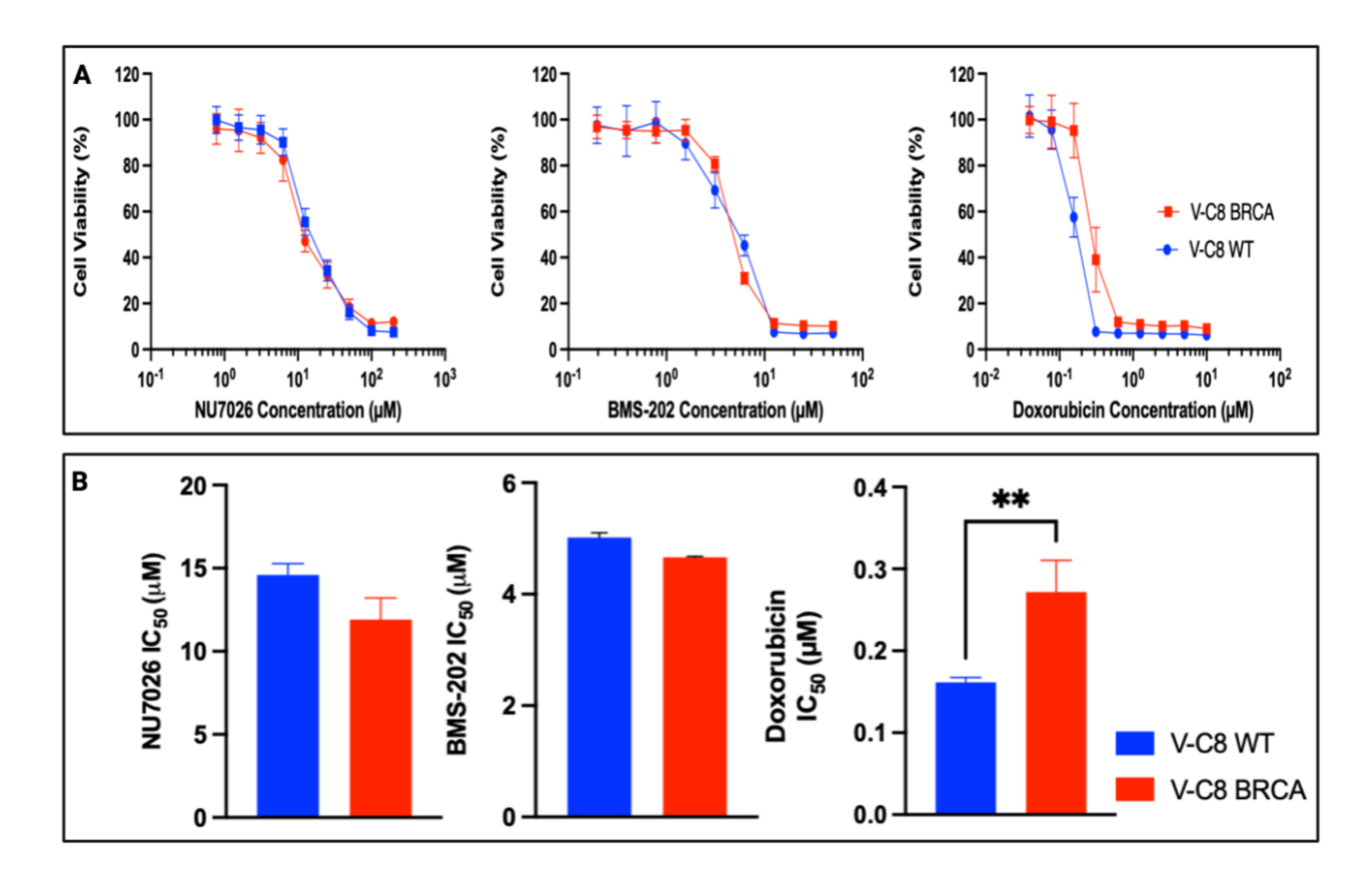


Figure 20: NU7026, BMS-202 and doxorubicin sensitivity in V-C8 WT and V-C8 BRCA cells. (A) Comparison of growth inhibition curves of NU7026, BMS-202 and doxorubicin in V-C8 WT and V-C8 BRCA cells. (B) Comparison of IC₅₀ values for each drug in the two cell lines.

The IC₅₀ of the individual drugs as well as the drugs in combination and the resulting CI₅₀ values are displayed in Figures 21C and 22C. Both BMS-202 and NU7026 demonstrated synergy with doxorubicin. Importantly, both synergistic combinations showed selectivity towards the V-C8 WT mutant cells as shown in the isobolograms displayed in Figures 21A and 22A.

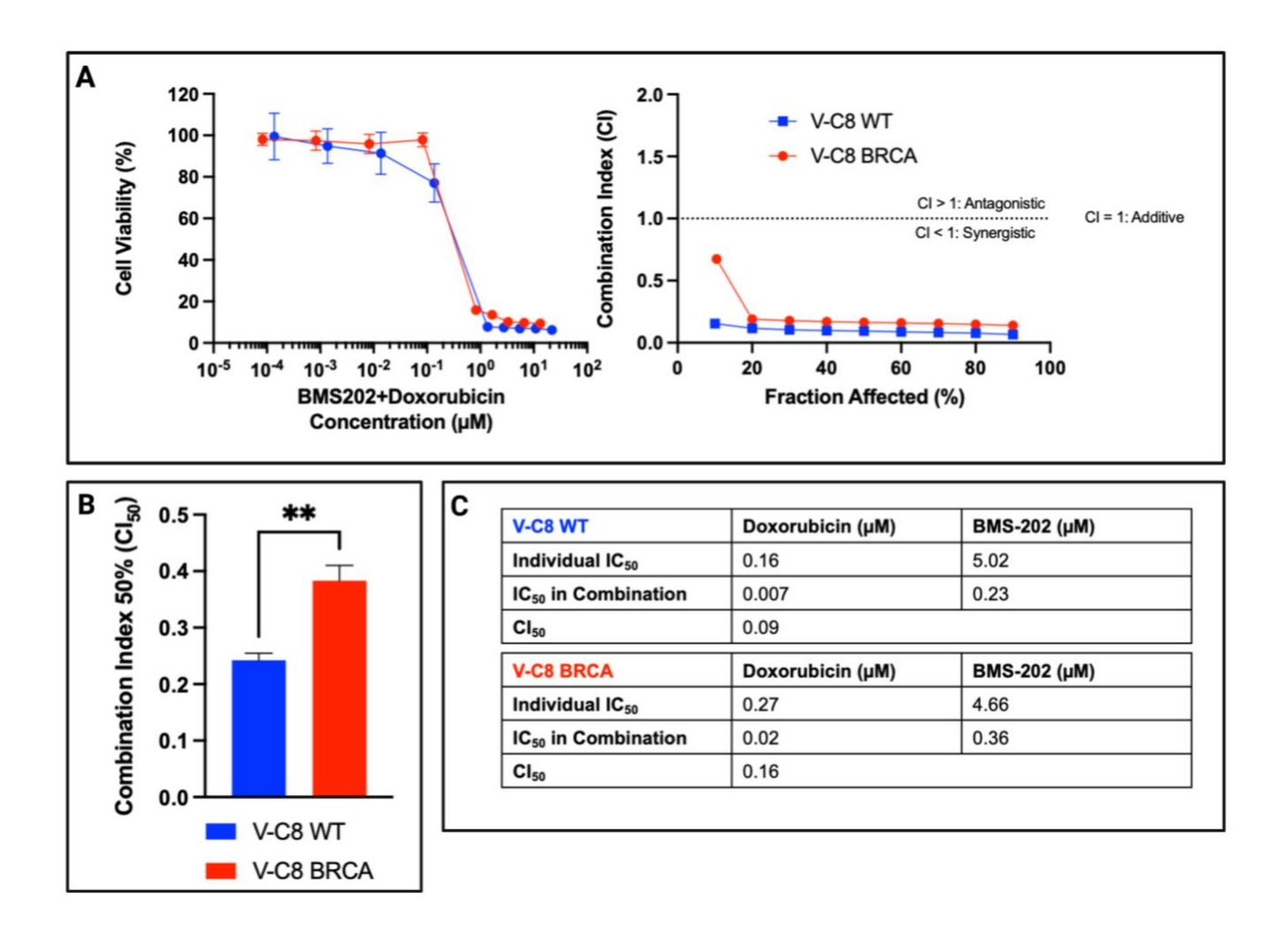


Figure 21: BMS-202 synergy with doxorubicin. (A) Growth inhibition curves (left) and corresponding isobologram (right) of a combination of BMS-202 and doxorubicin in V-C8 WT and V-C8 BRCA cells. (B) Comparison of CI₅₀ values for BMS-202 and doxorubicin in each cell line. (C) Individual IC₅₀, combination IC₅₀, and CI₅₀ values for each cell line.

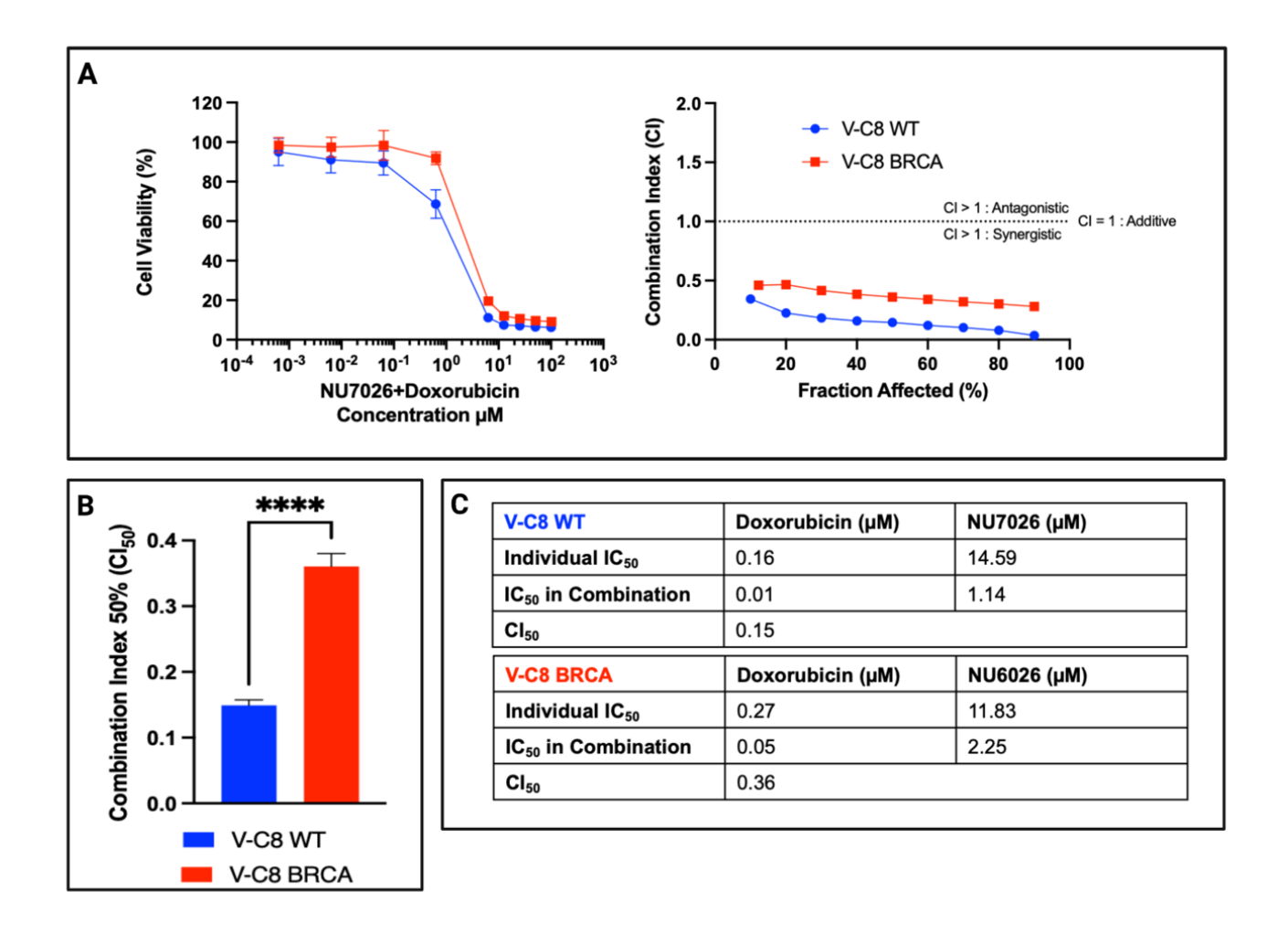


Figure 22: NU7026 synergy with doxorubicin. (A) Growth inhibition curves (left) and corresponding isobologram (right) of a combination of NU7026 and doxorubicin in V-C8 WT and V-C8 BRCA cells. (B) Comparison of CI₅₀ values for NU7026 and doxorubicin in each cell line. (C) Individual IC₅₀, combination IC₅₀, and CI₅₀ values for each cell line.

The shared synergy that BMS-202 and NU7026 displayed with doxorubicin between both cell lines, as well as their selective synergy to the WT mutant cells, supports a possible shared target between the drugs as revealed by the AF147 identification of DNA-PKcs as a BMS-202 binding partner.

AF147 detects change in binding profile following SAOS-2 multiple dose exposure to BMS-202

SAOS-2 cells were analyzed for their BMS-202 IC₅₀, relative PD-L1 levels, and AF147 binding signature before (P₀) and after (P₁₀) multiple dose exposure to 0.1μM BMS-202 over ten passages. The IC₅₀ value of BMS-202 decreased from 13.6μM at P₀ to 9.1μM at P₁₀, indicating that BMS-202 became more potent as the cells were exposed to the drug (Figure 23A). Additionally, the relative PD-L1 levels increased about 9 times over the ten passages (Figure 23B). These changes correlated to a changed BMS-202 binding profile identified by AF147 for the P₁₀ cells. The most prominent proteins detected from the P₀ cells, except for DNA-PKcs, were lost from the P₁₀ BMS-202 binding signature (Figure 23C).

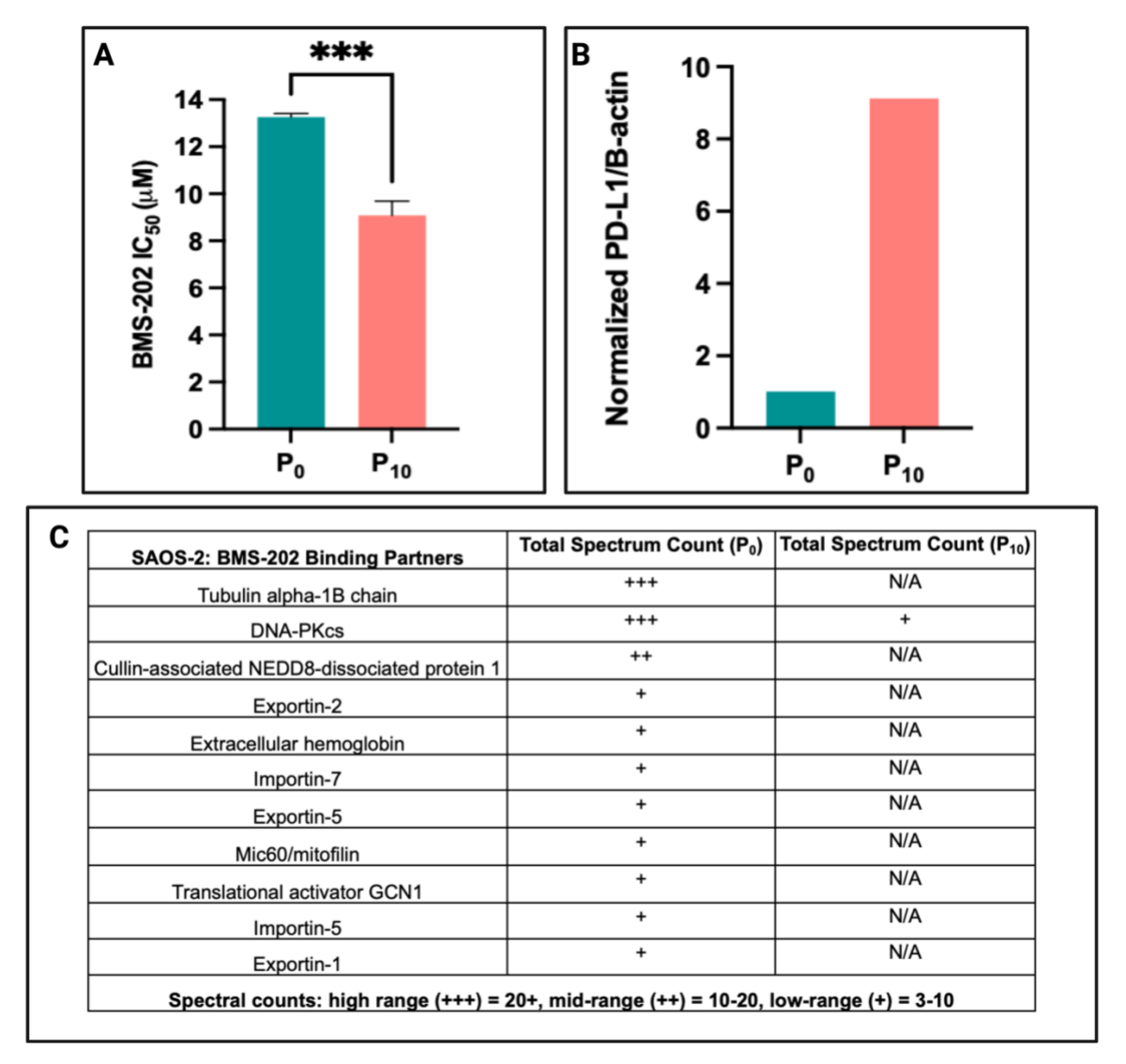


Figure 23: AF147 detects change in BMS-202 binding signature in SAOS-2 cells following their prolonged exposure to BMS-202. (A) Comparison of BMS-202 IC₅₀ values for P₀ and P₁₀ SAOS-2 cells. (2) Comparison of relative PD-L1 levels in P₀ and P₁₀ cells. (C) Comparison of BMS-202 binding signature in P₀ and P₁₀ cells. N/A indicates that the protein was not detected. An explanation of Scaffold generated proteomic data can be found in the description of Table 2.

DISCUSSION

The biorthogonal nature of the chemical probes maintains the integrity of their parent drug activity and allows them to be significant tools for research and clinical purposes. Although AF147 and AF219 were not able to capture PD-L1, the primary target of BMS-202, AF147 did show substantial interaction with it through the HTRF assay that involves PD-1/PD-L1 interaction.

Furthermore, AF147 was able to pulldown proteins implicated in malignancies indicating that its warhead is capable of actively targeting proteins involved in the biological processes of its parent drug. DNA-PKcs was a prominent binding partner in both SAOS-2 and A549 WT cells. It comprises DNA-PK, which is an essential enzyme in NHEJ-mediated DSB repairs. DNA-PK inhibitors have been shown to sensitize cancer cells to doxorubicin and ionizing radiation by increasing the persistence of their DSBs through prevention of their repair by NHEJ. DNA-PK

It was expected that targeting an additional binding partner of BMS-202, i.e. using NU7026 to target DNA-PK, would potentiate its activity. However, this was not demonstrated in SAOS-2, V-C8 WT or V-C8 BRCA cells. It is known that BRCA is synthetically lethal with PARP1 because BRCA deficient cells utilize PARP as the compensatory DDR pathway, therefore inhibition of PARP leads to cell death.³⁴ Having found that DNA-PK is a target for the BMS-202 scaffold, we attempted to verify whether it would be synthetically lethal with PARP. Thus, we designed experiments wherein BMS-202 was combined with a specific inhibitor of DNA-PK. We did not find any potentiation of BMS-202 whether it was with BRCA deficient cells or otherwise. Clearly, the combination of BMS-202 with NU7026 did not synergize with PARP. This suggests that perhaps BMS-202 is not targeting players in SSBs, like PARP1 inhibitors such as olaparib, or players in HR. Likewise, the effect of NU7026 did not indicate involvement of the latter with SSB.³³

Furthermore, both inhibitors displayed synergy with the DSB inducing chemotherapy, as indicated by all combinations at all doses used in combination with doxorubicin, a drug that is known to primarily act through DSB induction.⁷¹ Inhibition of DSB repair has already been shown to sensitize tumor cells to doxorubicin in many studies.^{67,69,71,75}

Our study gives prima facie evidence that our chemical probe can capture targets leading to the identification of molecules capable of synergizing with standard of care drugs. However, further work is required to confirm the interaction of BMS-202 with DNA-PK at the molecular level.

CHAPTER 3

CHAPTER 3: PROFILING BIOLOGICAL SYSTEMS WITH A CHEMICAL PROBE CARRYING A BETA-LACTAM SCAFFOLD: APPLICATION TO DRUG ALLERGY

INTRODUCTION

Prevalence and Implications of a Penicillin Allergy

Patient-reported AALs are most reported with penicillin β-lactams.⁵⁹ Their prevalence ranges from 6 to 25% across different areas and patient populations.⁴⁹ However, these labels are generally inappropriately assigned due to reactions misclassified as an antibiotic allergy and remain untested in medical settings.⁴⁹ It has been well documented that majority of patients with a penicillin AAL can in fact tolerate the antibiotics upon proper assessment.^{46,49}

The misuse of a penicillin AAL has individual and public health implications including increased use of suboptimal second-line or broader-coverage and more costly antimicrobials, increased ADEs, more postoperative surgical-site infections, increased risk of antibiotic resistance, and higher healthcare costs resulting from longer hospital stays. He costly implications of a misused AAL provide the rationale for penicillin allergy delabeling, which is a procedure for thoroughly assessing the validity of a label, as a strategy to improve antibiotic utilization and patient outcomes. He misused AAL provide the rationale for penicillin allergy delabeling to improve antibiotic utilization and patient outcomes.

Recent guidelines suggest the use of skin testing and/or DPTs to accurately assess a patient AAL.^{46,49} The optimal strategy to use is based on stratification of patients into low, moderate, and high risk of ADRs. There is a need for studies and tools that can help in risk stratification guidelines to increase the safety and accuracy of delabeling.⁶⁴ The use of a chemical probe may allow for safe and feasible ex vivo detection of molecular determinants that can aid in the proper risk stratification for patients.

Open- and Closed- Beta-Lactam Ring Chemical Probes

The probes contain a small molecule drug scaffold as a warhead and a biotin tail designed to be captured with streptavidin-coated magnetic beads and are designed to be used as a target profiling tool for their respective parent drug.^{4,9} The probes were synthesized with two biorthogonal functional groups consisting of an azide-warhead and a cyclooctyne biotin-PEG body to maintain the biological activity of the parent drug.⁹ Two chemical probes equipped with warheads derived from the penicillin antibiotic, ampicillin, were used for this study (Figures 24 and 25). AF132 has an ampicillin warhead with a closed β -lactam ring while AF239 has an ampicillin warhead with an open β -lactam ring. Their azide-warhead components, AF130 and AF238, respectively, were used as well. AB22, a chemical probe synthesized with a cyclohexane nonspecific warhead, was used as the negative control probe.

Figure 24: Closed \beta-lactam ring structures. Chemical structures of AF132 and AF130. β -lactam antibiotic scaffold is highlighted in red.

Figure 25: Open β-lactam ring structures. Chemical structures of AF239 and AF238. β -lactam antibiotic scaffold is highlighted in red.

The closed β -lactam ring is the form of the drug administered to patients and is considered a minor determinant of allergy whereas the open form, or the penicilloyl metabolite, is the antigenic intermediate generated in vivo and is considered the major determinant of an allergy. ⁴⁹⁻⁵¹ The two probes were used against human serum to assess their ability to capture β -lactam specific IgE. The serum of two samples with DPT confirmed penicillin allergies as well as the serum of two control samples - one peanut-allergy as the non-penicillin allergic control and one sample with no reported allergies as the non-allergic control - were assessed in this study.

METHODS AND MATERIALS

Chemical Probe Preparation

The chemical probes, AF132 and AF239, in addition to their azide warhead components, AF103 and AF238, respectively, as well as AB22, were all synthesized in our laboratory. Stock solutions (10-25mM) of all molecules were prepared in DMSO under sterile conditions. All stock solutions were diluted to 10µM in accordance with the magnetic bead pulldown protocol.

Magnetic Bead Pulldown with Chemical Probe

The serum samples for challenging our chemical probes were obtained from the laboratory of Dr. Christos Tsoukas (Division of Allergy & Immunology; REB Approval: 2018-3852) and the control samples, which include a peanut allergy, were obtained from the laboratory of Dr. Bruce Mazer (Division of Allergy/Immunology/Dermatology). AF132, AF239, AF130, and/or AF238 were prepared as 10µM solutions and then pre-immobilized onto streptavidin magnetic beads (ThermoFisher Scientific, Waltham, MA, USA). A chloroform (ThermoFisher Scientific) lipid extraction was performed on the serum samples in which a 1:1 ratio of chloroform:serum was

centrifuged at 15000rpm for 15min. A supernatant volume of 50µL was incubated with the magnetic beads for 2 hours. If AF130 and/or AF238 were used, 10µM of AF103 was added to the respective sample for an additional two-hour incubation to complete the SPAA reaction. The mixture was agitated with a tube rotator during the incubation period to facilitate the binding of the probe warhead to its binding partners and/or the binding of the azide warhead to AF103. The beads were then cleared of excess solvent and washed before proceeding with the western blot analysis of the captured proteins. An illustration of this process is shown in Figure 13.

Western Blot

30μL of 2x Laemmli Sample Buffer (BioRad, Hercules, CA, USA) was used at this stage to elute the captured proteins from the magnetic beads following the pulldowns. The samples were loaded and resolved on 10% SDS-PAGE and then transferred to a PVDF membrane (Bio-Rad). Membranes were blocked with 5% BSA in 0.1% PBST for 45min at room temperature prior to an overnight incubation at 4°C with an anti-human IgE antibody (Bethyl Laboratories, Montgomery, TX, USA) diluted 1:20000 in 5% BSA in 0.1% PBST. The membranes were then washed three times with 0.2% PBST and incubated for one hour at room temperature with streptavidin-horseradish peroxidase (BioLegend, San Diego, CA, USA) diluted 1:3000 in 1% BSA in 0.2% PBST. After three more washes with 0.2% PBST, the presence or absence of IgE was determined using PierceTM ECL Western Blotting Substrate (ThermoFisher Scientific).

RESULTS

AF132 and AF239 capture IgE from penicillin-allergic serum

to detect the presence or absence of IgE.

The serum samples of two DPT confirmed penicillin allergies and the control serum samples, including both a peanut allergy and no reported allergies, were used for chemical probe pulldowns with AF132, AF239 and AB22. The captured proteins were then analyzed via western blot for the presence of IgE (Figure 26).

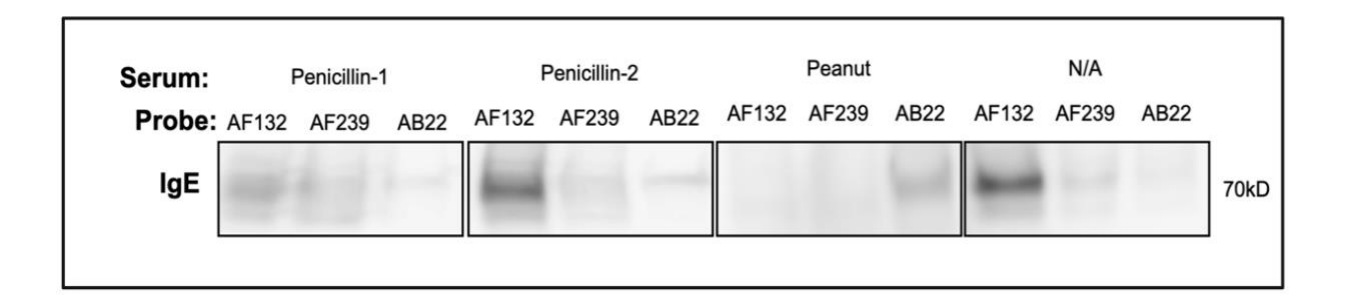


Figure 26: IgE detection in serum via western blot analysis on chemical probe-captured proteins. Chemical probe pulldowns using AF132, AF239, and AB22 were completed on two different penicillin allergic serum samples (penicillin-1 and penicillin-2), a peanut allergic serum sample and a serum sample with no known allergies (N/A). The captured proteins from each pulldown were analyzed via western blot

AF132 and AF239 have warheads derived from ampicillin; therefore, it can be inferred that the western blot signals represent IgE specific to \(\beta\)-lactams because the serum proteins that do not attach to the probes are washed away (Figure 13). AF132 has a clearer signal for IgE than AF239 in both penicillin allergic samples, but it is not possible to claim it captured more IgE per sample since a loading control was not available for the serum samples in this study. A faint signal was detected by AB22, which does not have a targeted warhead, and this may correlate to nonspecific binding of IgE along the shared biotin-PEG moiety of all probes. AF132 and AF239 did not

generate IgE signals in the serum sample from a peanut allergy, which supports the specificity of the probes. However, a strong signal for IgE was detected by AF132 from the sample with no known allergies.

AF130 and AF238 maintain activity of respective reagent probe

A pulldown was completed with AF130 and AF238, the biorthogonal, complementary functional parts of AF132 and AF239, respectively, to evaluate whether the warheads captured IgE differently without AF103, the biotin-PEG moiety of the probe. The serum sample labeled "penicillin-2" was used for this analysis because the clear signals it generated with the reagent probes would allow for more accurate evaluation of results (Figure 27).

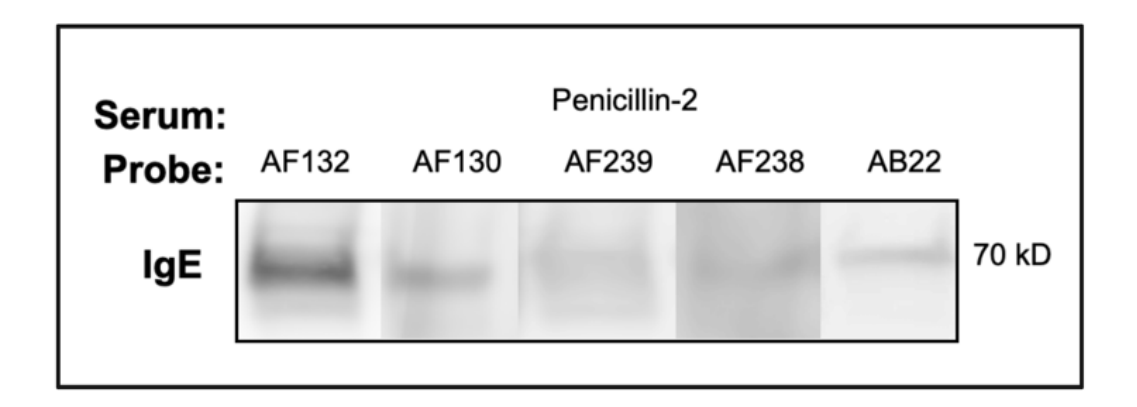


Figure 27: Comparison of IgE detection between reagent probe and biorthogonal components via western blot analysis. Chemical probe pulldowns using the reagent probes, AF132 and AF239, as well as their azide-warheads, AF130 and AF238, respectively, were completed on the penicillin-2 allergic sample. The captured proteins from each pulldown were analyzed via western blot to detect the presence or absence of IgE.

AF130 and AF238 appear to generate similar signals as their respective reagent probe with AF130 generating a stronger signal than AF238. The proper loading control, such as the protein transferrin for serum samples, to interpret the western blot results more thoroughly was not available.⁷⁶ Additionally, correlating the western blot quantification with a measure of total IgE in the serum sample via an ELISA would have provided better insight into the mechanisms of β-lactam allergy.

DISCUSSION

The initial studies completed with the penicillin-equipped chemical probes suggest that they may be able to capture proteins implicated in an antibiotic allergy from patient serum. The closed β -lactam ring of AF132 appears to have interacted more strongly with IgE than the open β -lactam ring of AF239. Their biorthogonal components, AF130 and AF238, respectively, generate comparable results suggesting that all forms of the probe interact similarly with IgE. The signals generated by AB22 may be explained by nonspecific IgE binding along the body of the probe, which is a functional element shared with the experimental probes.

IgE was not detected from the peanut-allergic sample, which supports the specificity of the chemical probes for penicillin-specific IgE. However, the detection of IgE from a sample with no reported allergies raises a question on specificity. A greater sample size for both penicillin-allergic serum and non-penicillin allergic/no allergy serum is necessary to further understand and validate these findings.

The preliminary data generated from the probes indicates that they may be able to interact with endogenous proteins that give rise to an allergy. The identification of these proteins via

proteomic analysis may provide information on molecular determinants of allergy that can be used to assist in patient stratification efforts to properly evaluate the validity of a penicillin AAL.

CHAPTER 4

CHAPTER 4: DISCUSSION AND CONTRIBUTION TO KNOWLEDGE

The field of drug target profiling is rapidly evolving, and novel approaches are being developed to assess proteomic based drug response.⁷⁷ The novel chemical probes presented in this study were designed to address the need of target profiling small molecule drug scaffolds. Targets identified from the profiles are potentially usable for therapeutic intervention and diagnostic purposes. Here, our study evaluated scaffolds derived from BMS-202, a small molecule PD-L1 inhibitor, and penicillin to explore binding profiles from biological systems.

IMMUNO-ONCOLOGY

BMS-202 interacts with PD-L1 as its primary target to obstruct its binding to PD-1.²¹ The first set of experiments using AF147 and AF219 were carried out to determine if, and to what extent, they could interact with and/or pulldown PD-L1. The strong binding of AF147 to PD-L1 was shown using the HTRF assay. However, western blot and proteomic analysis of the cell lysates did not show the capture of PD-L1. PD-L1 was absent from every pulldown conducted with AF147.

The PD-L1 signal generated at 50kD for SAOS-2 cells and at 75kD for NIH WT and A549 WT cells is likely a result of glycosylation, which often yields heterogenous protein patterns on western blots. A previous study demonstrated that PD-L1 of cancer cells is heavily glycosylated and treatment with glycosidase, which removed the glycan structure of PD-L1, reduced a significant amount of previously 45kD PD-L1 to a lower molecular weight of 33kD. Previous research has also shown that glycosylation of PD-L1 does not sterically interfere with its dimerization by BMS-202. Therefore, it does not seem that the glycosylation shown in these cell lines is contributing to the inability of AF147 to capture PD-L1.

The addition of exogenous PD-L1, which was presumed to facilitate greater interaction between AF147 and PD-L1, did not assist in its capture by the probe. Control serum, which was employed to test AF147 in its clinically equivalent biological milieu, similarly did not generate any positive results.

The biorthogonal approach for probing a biological sample consists of exposing the biological system to the click acceptor followed by a pulldown with the click donor. AF219 acts as the click acceptor, and AF103 acts as the click donor to facilitate target capture. Even under such conditions, PD-L1 was not captured.

The retention of BMS-202 activity by the probes was supported through the large increase in SAOS-2 PD-L1 levels over the course of a 6-hour AF219 treatment. Previous studies have shown that transient increases in PD-L1 levels by anti-PD-L1 molecules are followed by its downregulation through cell internalization.⁷³ While further insight into BMS-202 mechanism of action is needed to understand what drove the increase, the change indicates that probe synthesis did not disrupt the activity of BMS-202. Additionally, BMS-202 induces PD-L1 dimerization to occlude its binding to PD-1; it is possible that the conditions and biological machinery that enable dimerization were not maintained in the completed experiments, thereby preventing PD-L1 capture by the probes.²¹ These reasons supported further analysis using AF147 as a tool to identify secondary targets of BMS-202.

AF147 identified several potential binding partners for SAOS-2 and A549 WT cells that have been implicated in different malignancies and cancer-related processes (Table 3). Its ability to capture these proteins supports the possibility that AF147 can be a useful tool for understanding cellular interactions associated with the BMS-202 scaffold. Cross-validation of these proteins using western blot analysis would further confirm these target interactions.

Table 3: Prominent BMS-202 binding partners implicated in different cancers and cancer-related processes.

BMS-202 Binding Partners	Implicated Cancer/Process
DNA-PKcs	Anti-cancer drug resistance
Tubulin alpha-1B chain	Anti-cancer drug resistance
Translational activator GCN1	Prostrate cancer
Mic60/mitofilin	Pancreatic, gastric and prostate cancer
Cullin-associated NEDD8-dissociated protein 1	Prostrate cancer
Nuclear transport proteins (exportins and importins)	Tumorigenesis and anti-cancer drug resistance

The implicated cancer or cancer-related process of the most prominent BMS-202 binding partners identified through an AF147 pulldown on SAOS-2 and A549 WT cells.⁷⁹⁻⁸⁴

DNA-PKcs was the most prominent binding partner under all probing conditions. Therefore, it was important to explore its relationship to PD-L1. The latter has been connected to DSBs and DDR, and DNA-PKcs has been implicated in immunotherapies. A novel synthetically lethal relationship between PD-L1 and DNA-PK was recently demonstrated in triple-negative breast cancer. These factors helped identify DNA-PKcs as a probable binding partner of BMS-202 and encouraged its further investigation.

Neither BMS-202 nor NU7026 displayed selective potency towards the V-C8 WT mutant cells, which suggests that neither PD-L1 nor DNA-PK have synthetically lethal interactions with BRCA2 or are involved in DNA SSB repair. Indeed, the data suggest that both proteins may not be involved in the compensatory SSB repair pathway of the WT mutant and may share involvement in DSBs. This was further investigated on V-C8 WT and V-C8 BRCA cell lines through determining whether BMS-202 and NU7026 exhibit synergy with doxorubicin, a chemotherapeutic agent that generates DNA DSBs by targeting DNA topoisomerase II.⁷¹ We

expected that BMS-202 potentiation of the latter drug may suggest its interaction with mechanisms related to DNA DSB repair perhaps associated with DNA-PK. Both drugs synergized with doxorubicin at all concentrations tested, supporting the notion that BMS-202 may act on targets involved in DNA DSB.

Previous studies have demonstrated that targeting DNA-PK sensitizes colon, prostate, and breast cancer cells to doxorubicin and ionizing radiation by increasing the persistence of DSBs through prevention of their NHEJ-mediated repair. Additionally, a recent in vivo study found that the treatment of a DNA-PK inhibitor in combination with radiation established immunologic memory that delayed or prevented colon tumor growth in rechallenged mice. Similarly, combinations between chemotherapies and immunotherapies are also being pursued due to evidence of chemotherapy induced immunogenic cell death sensitizing TMEs to immune checkpoint blockade. A significant body of work has therefore been accumulated to show the synergistic relationship identified in the V-C8 WT and BRCA cells. Accordingly, the established synergy highlights the innovative way in which a binding signature generated by the chemical probe can lead to the rational design of synergistic combinations. The molecular basis of the synergistic interaction between BMS-202 and doxorubicin is awaiting further investigation.

It is noteworthy to emphasize the synergistic growth inhibition exerted by doxorubicin with BMS-202 and NU7026 occurs at a significant reduction in their IC₅₀ values when used in combination versus when used individually. This suggests that such a combination could be used to reduce drug toxicity of doxorubicin.

Given the potential clinical advantage of the combination between BMS-202 and doxorubicin, it is worth investing the physical interactions between BMS-202 and DNA-PK through X-ray crystallography and/or computational methods of molecular modeling. Such

analyses of BMS-202 in complex with DNA-PK, as well as NU7026 in complex with PD-L1, would be useful to explore the ways in which chemical probes can be used in drug development and optimization.

DRUG ALLERGY

The initial studies completed with the β-lactam probes similarly provided a case for the potential of the chemical probe approach highlighted in this study. Although additional investigation is necessary to validate and understand the findings, it appears that the closed β-lactam ring of the parental ampicillin more strongly interacted with IgE than the open β-lactam ring of the penicilloyl derivative. Like AF147 and AF219, the activity of the biorthogonal components of AF132 and AF239 generated the same results as their reagent probe.

No IgE capture from the peanut allergic serum supports the specificity of AF132 and AF239 for IgE raised against penicillin, however the detection of a signal from the serum with no known allergies was unexpected. The serum sample size for these studies was too small to draw any valid conclusions, and more samples are necessary to properly assess the efficacy of the probes.

Further validation of the chemical probe pulldown requires a larger sample size of serum samples. The observations in this thesis set premise for further analysis in the larger sample size. Indeed, this work will continue under the iDEAL protocol (DIagnostic anD predictor Tools for Immune-mediated Drug ALlergy – A prospective multicenter cohort study). These studies aim to identify secondary protein targets of β-lactams and their antigenic contribution to an allergic response. Understanding the molecular determinants of allergy may provide a safe, ex vivo method

to more accurately and safely stratify patients with an AAL into the appropriate risk category for evaluation of their allergy.

CONCLUSION

The preliminary studies presented in this thesis are a proof-of-concept of the rationale for the novel chemical probe approach detailed throughout this work. The chemical probes displayed potential and similar use across two areas of study in which innovation is needed to advance research, therapeutics, and diagnostics.

The immuno-oncology and drug allergy probes demonstrated maintenance of their parent drug targeting through inhibition of PD-1/PD-L1 binding and the apparent capture of penicillin-specific IgE from serum, respectively. Furthermore, the identification of several BMS-202 cancer-related binding partners demonstrated that chemical probes may be capable of detecting molecular targets that inspire drug combinations. Analysis of the signatures led to the identification of a new target for BMS-202 that can be used to potentiate the action of doxorubicin, a standard of care drug used in the clinical management of advanced cancers. The binding signature was used to identify potential synergy between drug combinations, which indicates that chemical probes can be an innovative way to explore pharmacological interactions.

Additional research is needed for the validation and expansion of the conclusions drawn throughout this project. The chemical probes provided preliminary evidence that they may be tools capable of defining critical targets from biological fluids that can be used for therapeutic intervention. This can extend their benefit to improve therapeutic and diagnostic development.

REFERENCES

- 1. Chen X, Wang Y, Ma N, et al. Target identification of natural medicine with chemical proteomics approach: probe synthesis, target fishing and protein identification. *Signal Transduction and Targeted Therapy*. 2020/05/21 2020;5(1):72. doi:10.1038/s41392-020-0186-y
- 2. Wright MH, Sieber SA. Chemical proteomics approaches for identifying the cellular targets of natural products. 10.1039/C6NP00001K. *Natural Product Reports*. 2016;33(5):681-708. doi:10.1039/C6NP00001K
- 3. Wang S, Tian Y, Wang M, Wang M, Sun GB, Sun XB. Advanced Activity-Based Protein Profiling Application Strategies for Drug Development. *Front Pharmacol.* 2018;9:353. doi:10.3389/fphar.2018.00353
- 4. Fonović M, Bogyo M. Activity-based probes as a tool for functional proteomic analysis of proteases. *Expert Rev Proteomics*. 2008;5(5):721-730. doi:10.1586/14789450.5.5.721
- 5. Cooper MJ, Cox NJ, Zimmerman EI, et al. Application of multiplexed kinase inhibitor beads to study kinome adaptations in drug-resistant leukemia. *PLoS One*. 2013;8(6):e66755. doi:10.1371/journal.pone.0066755
- 6. Cousins EM, Goldfarb D, Yan F, et al. Competitive Kinase Enrichment Proteomics Reveals that Abemaciclib Inhibits GSK3β and Activates WNT Signaling. *Mol Cancer Res*. Feb 2018;16(2):333-344. doi:10.1158/1541-7786.Mcr-17-0468
- 7. Duncan JS, Whittle MC, Nakamura K, et al. Dynamic reprogramming of the kinome in response to targeted MEK inhibition in triple-negative breast cancer. *Cell.* Apr 13 2012;149(2):307-21. doi:10.1016/j.cell.2012.02.053
- 8. Klaeger S, Heinzlmeir S, Wilhelm M, et al. The target landscape of clinical kinase drugs. *Science*. Dec 1 2017;358(6367)doi:10.1126/science.aan4368

- 9. Bird RE, Lemmel SA, Yu X, Zhou QA. Bioorthogonal Chemistry and Its Applications. *Bioconjugate Chemistry*. 2021/12/15 2021;32(12):2457-2479. doi:10.1021/acs.bioconjchem.1c00461
- 10. Sletten EM, Bertozzi CR. Bioorthogonal Chemistry: Fishing for Selectivity in a Sea of Functionality. *Angewandte Chemie International Edition*. 2009;48(38):6974-6998. doi:https://doi.org/10.1002/anie.200900942
- 11. Wang J, Zhang C-J, Chia WN, et al. Haem-activated promiscuous targeting of artemisinin in Plasmodium falciparum. *Nature Communications*. 2015/12/22 2015;6(1):10111. doi:10.1038/ncomms10111
- 12. Fouad YA, Aanei C. Revisiting the hallmarks of cancer. *Am J Cancer Res*. 2017;7(5):1016-1036.
- 13. Philips GK, Atkins M. Therapeutic uses of anti-PD-1 and anti-PD-L1 antibodies. *International Immunology*. 2014;27(1):39-46. doi:10.1093/intimm/dxu095
- 14. Akinleye A, Rasool Z. Immune checkpoint inhibitors of PD-L1 as cancer therapeutics. *J Hematol Oncol*. Sep 5 2019;12(1):92. doi:10.1186/s13045-019-0779-5
- 15. Amornsupak K, Thongchot S, Thinyakul C, et al. HMGB1 mediates invasion and PD-L1 expression through RAGE-PI3K/AKT signaling pathway in MDA-MB-231 breast cancer cells. *BMC Cancer*. 2022/05/24 2022;22(1):578. doi:10.1186/s12885-022-09675-1
- 16. Rojas A, Schneider I, Lindner C, Gonzalez I, Morales MA. The RAGE/multiligand axis: a new actor in tumor biology. *Biosci Rep.* Jul 29 2022;42(7)doi:10.1042/bsr20220395
- 17. Gong J, Chehrazi-Raffle A, Reddi S, Salgia R. Development of PD-1 and PD-L1 inhibitors as a form of cancer immunotherapy: a comprehensive review of registration trials and future considerations. *J Immunother Cancer*. 2018;6(1):8. doi:10.1186/s40425-018-0316-z

- 18. Vaddepally RK, Kharel P, Pandey R, Garje R, Chandra AB. Review of Indications of FDA-Approved Immune Checkpoint Inhibitors per NCCN Guidelines with the Level of Evidence. *Cancers (Basel)*. 2020;12(3):738. doi:10.3390/cancers12030738
- 19. Basu S, Yang J, Xu B, et al. Design, Synthesis, Evaluation, and Structural Studies of C2-Symmetric Small Molecule Inhibitors of Programmed Cell Death-1/Programmed Death-Ligand 1 Protein–Protein Interaction. *Journal of Medicinal Chemistry*. 2019/08/08 2019;62(15):7250-7263. doi:10.1021/acs.jmedchem.9b00795
- 20. Yang J, Hu L. Immunomodulators targeting the PD-1/PD-L1 protein-protein interaction: From antibodies to small molecules. *Medicinal Research Reviews*. 2019;39(1):265-301. doi:https://doi.org/10.1002/med.21530
- 21. Zak KM, Grudnik P, Guzik K, et al. Structural basis for small molecule targeting of the programmed death ligand 1 (PD-L1). *Oncotarget*. 2016;7(21)
- 22. Del Gatto A, Cobb SL, Zhang J, Zaccaro L. Editorial: Peptidomimetics: Synthetic Tools for Drug Discovery and Development. Editorial. *Frontiers in Chemistry*. 2021-November-12 2021;9doi:10.3389/fchem.2021.802120
- 23. Chupak LS, Zheng, Xiaofan, inventor; Compounds useful as immunomodulators. 2015.
- 24. Ashizawa T, Iizuka A, Tanaka E, et al. Antitumor activity of the PD-1/PD-L1 binding inhibitor BMS-202 in the humanized MHC-double knockout NOG mouse. *Biomed Res*. 2019;40(6):243-250. doi:10.2220/biomedres.40.243
- 25. Hu Z, Yu P, Du G, et al. PCC0208025 (BMS202), a small molecule inhibitor of PD-L1, produces an antitumor effect in B16-F10 melanoma-bearing mice. *PloS one*. 2020;15(3):e0228339-e0228339. doi:10.1371/journal.pone.0228339

- 26. Zhang H, Xia Y, Yu C, et al. Discovery of Novel Small-Molecule Inhibitors of PD-1/PD-L1 Interaction via Structural Simplification Strategy. *Molecules*. 2021;26(11):3347.
- 27. Alsaab HO, Sau S, Alzhrani R, et al. PD-1 and PD-L1 Checkpoint Signaling Inhibition for Cancer Immunotherapy: Mechanism, Combinations, and Clinical Outcome. Review. *Frontiers in Pharmacology*. 2017-August-23 2017;8doi:10.3389/fphar.2017.00561
- 28. Chatterjee N, Walker GC. Mechanisms of DNA damage, repair, and mutagenesis. *Environ Mol Mutagen*. Jun 2017;58(5):235-263. doi:10.1002/em.22087
- 29. Burgess JT, Rose M, Boucher D, et al. The Therapeutic Potential of DNA Damage Repair Pathways and Genomic Stability in Lung Cancer. Review. *Frontiers in Oncology*. 2020-July-28 2020;10doi:10.3389/fonc.2020.01256
- 30. Hegde ML, Hazra TK, Mitra S. Early steps in the DNA base excision/single-strand interruption repair pathway in mammalian cells. *Cell Research*. 2008/01/01 2008;18(1):27-47. doi:10.1038/cr.2008.8
- 31. Huang R, Zhou P-K. DNA damage repair: historical perspectives, mechanistic pathways and clinical translation for targeted cancer therapy. *Signal Transduction and Targeted Therapy*. 2021/07/09 2021;6(1):254. doi:10.1038/s41392-021-00648-7
- 32. Jean-Claude BJ. Chemosensitization to Platinum-Based Anticancer Drugs. In: Panasci LC, Alaoui-Jamali MA, eds. *DNA Repair in Cancer Therapy*. Humana Press; 2004:51-71.
- 33. Yue X, Bai C, Xie D, Ma T, Zhou P-K. DNA-PKcs: A Multi-Faceted Player in DNA Damage Response. Review. *Frontiers in Genetics*. 2020-December-23 2020;11doi:10.3389/fgene.2020.607428

- 34. Rose M, Burgess JT, O'Byrne K, Richard DJ, Bolderson E. PARP Inhibitors: Clinical Relevance, Mechanisms of Action and Tumor Resistance. Review. *Frontiers in Cell and Developmental Biology*. 2020-September-09 2020;8doi:10.3389/fcell.2020.564601
- 35. O'Connor MJ. Targeting the DNA Damage Response in Cancer. *Mol Cell*. Nov 19 2015;60(4):547-60. doi:10.1016/j.molcel.2015.10.040
- 36. Dobzhansky T. Genetics of natural populations; recombination and variability in populations of Drosophila pseudoobscura. *Genetics*. May 1946;31(3):269-90. doi:10.1093/genetics/31.3.269
- 37. Murata MM, Kong X, Moncada E, et al. NAD+ consumption by PARP1 in response to DNA damage triggers metabolic shift critical for damaged cell survival. *Mol Biol Cell*. Sep 15 2019;30(20):2584-2597. doi:10.1091/mbc.E18-10-0650
- 38. Li X, Heyer W-D. Homologous recombination in DNA repair and DNA damage tolerance. *Cell Research*. 2008/01/01 2008;18(1):99-113. doi:10.1038/cr.2008.1
- 39. Cousineau I, Abaji C, Belmaaza A. BRCA1 Regulates RAD51 Function in Response to DNA Damage and Suppresses Spontaneous Sister Chromatid Replication Slippage: Implications for Sister Chromatid Cohesion, Genome Stability, and Carcinogenesis. *Cancer Research*. 2005;65(24):11384-11391. doi:10.1158/0008-5472.Can-05-2156
- 40. Xing J, Wu X, Vaporciyan AA, Spitz MR, Gu J. Prognostic significance of ataxia-telangiectasia mutated, DNA-dependent protein kinase catalytic subunit, and Ku heterodimeric regulatory complex 86-kD subunit expression in patients with nonsmall cell lung cancer. *Cancer*. 2008;112(12):2756-2764. doi:https://doi.org/10.1002/cncr.23533

- 41. Topatana W, Juengpanich S, Li S, et al. Advances in synthetic lethality for cancer therapy: cellular mechanism and clinical translation. *Journal of Hematology & Oncology*. 2020/09/03 2020;13(1):118. doi:10.1186/s13045-020-00956-5
- 42. Patterson-Fortin J, Bose A, Tsai W-C, et al. Targeting DNA Repair with Combined Inhibition of NHEJ and MMEJ Induces Synthetic Lethality in TP53-Mutant Cancers. *Cancer Research*. 2022;82(20):3815-3829. doi:10.1158/0008-5472.Can-22-1124
- 43. Ciszewski WM, Tavecchio M, Dastych J, Curtin NJ. DNA-PK inhibition by NU7441 sensitizes breast cancer cells to ionizing radiation and doxorubicin. *Breast Cancer Research and Treatment*. 2014/01/01 2014;143(1):47-55. doi:10.1007/s10549-013-2785-6
- 44. Zhao Y, Thomas HD, Batey MA, et al. Preclinical Evaluation of a Potent Novel DNA-Dependent Protein Kinase Inhibitor NU7441. *Cancer Research*. 2006;66(10):5354-5362. doi:10.1158/0008-5472.Can-05-4275
- 45. Bush K, Bradford PA. β-Lactams and β-Lactamase Inhibitors: An Overview. *Cold Spring Harb Perspect Med.* Aug 1 2016;6(8)doi:10.1101/cshperspect.a025247
- 46. Jeimy S, Ben-Shoshan M, Abrams EM, Ellis AK, Connors L, Wong T. Practical guide for evaluation and management of beta-lactam allergy: position statement from the Canadian Society of Allergy and Clinical Immunology. *Allergy, Asthma & Clinical Immunology*. 2020/11/10 2020;16(1):95. doi:10.1186/s13223-020-00494-2
- 48. Macy E. Penicillin and Beta-Lactam Allergy: Epidemiology and Diagnosis. *Current Allergy and Asthma Reports*. 2014/09/13 2014;14(11):476. doi:10.1007/s11882-014-0476-y

- 49. Castells M, Khan DA, Phillips EJ. Penicillin Allergy. *New England Journal of Medicine*. 2019;381(24):2338-2351. doi:10.1056/NEJMra1807761
- 50. Mayorga C, Montañez MI, Najera F, et al. The Role of Benzylpenicilloyl Epimers in Specific IgE Recognition. Original Research. *Frontiers in Pharmacology*. 2021-February-26 2021;12doi:10.3389/fphar.2021.585890
- 51. Bush K. CHAPTER 14 β-Lactam antibiotics: penicillins. In: Finch RG, Greenwood D, Norrby SR, Whitley RJ, eds. *Antibiotic and Chemotherapy (Ninth Edition)*. W.B. Saunders; 2010:200-225.
- 52. Wagle SSD, inventor; Lyophilized MDM composition and method of making it. patent application 89119819.4. 1990.
- 53. Trubiano JA, Chen C, Cheng AC, et al. Antimicrobial allergy 'labels' drive inappropriate antimicrobial prescribing: lessons for stewardship. *Journal of Antimicrobial Chemotherapy*. 2016;71(6):1715-1722. doi:10.1093/jac/dkw008
- 54. Marwa K, Kondamudi NP. Type IV Hypersensitivity Reaction. *StatPearls*. StatPearls Publishing

Copyright © 2022, StatPearls Publishing LLC.; 2022.

- 55. Illing PT, Mifsud NA, Purcell AW. Allotype specific interactions of drugs and HLA molecules in hypersensitivity reactions. *Current Opinion in Immunology*. 2016/10/01/2016;42:31-40. doi:https://doi.org/10.1016/j.coi.2016.05.003
- 56. Kostara M, Chondrou V, Sgourou A, Douros K, Tsabouri S. HLA Polymorphisms and Food Allergy Predisposition. *J Pediatr Genet*. Jun 2020;9(2):77-86. doi:10.1055/s-0040-1708521
- 57. Pichler WJ. Anaphylaxis to drugs: Overcoming mast cell unresponsiveness by fake antigens. *Allergy*. 2021;76(5):1340-1349. doi:https://doi.org/10.1111/all.14554

- 58. Aun MV, Kalil J, Giavina-Bianchi P. Drug-Induced Anaphylaxis. *Immunology and Allergy Clinics of North America*. 2017/11/01/ 2017;37(4):629-641. doi:https://doi.org/10.1016/j.iac.2017.06.002
- 59. De Luca JF, James F, Vogrin S, et al. Study protocol for PREPARE: a phase II feasibility/safety randomised controlled trial on PeRiopErative Penicillin AlleRgy TEsting. *BMJ Open.* 2023;13(2):e067653. doi:10.1136/bmjopen-2022-067653
- 60. Control CfD, Prevention. Evaluation and diagnosis of penicillin allergy for healthcare professionals: Is it really a penicillin allergy. 2017.
- 61. Trubiano JA. A Risk-Based Approach to Penicillin Allergy. *Immunology and Allergy Clinics of North America*. 2022/05/01/ 2022;42(2):375-389. doi:https://doi.org/10.1016/j.iac.2021.12.002
- 62. Mayorga C, Celik G, Rouzaire P, et al. In vitro tests for drug hypersensitivity reactions: an ENDA/EAACI Drug Allergy Interest Group position paper. *Allergy*. Aug 2016;71(8):1103-34. doi:10.1111/all.12886
- 63. Romano A, Atanaskovic-Markovic M, Barbaud A, et al. Towards a more precise diagnosis of hypersensitivity to beta-lactams an EAACI position paper. *Allergy*. Jun 2020;75(6):1300-1315. doi:10.1111/all.14122
- 64. Sousa-Pinto B, Tarrio I, Blumenthal KG, et al. Accuracy of penicillin allergy diagnostic tests: A systematic review and meta-analysis. *Journal of Allergy and Clinical Immunology*. 2021;147(1):296-308. doi:10.1016/j.jaci.2020.04.058
- 65. Herbst RS, Soria JC, Kowanetz M, et al. Predictive correlates of response to the anti-PD-L1 antibody MPDL3280A in cancer patients. *Nature*. Nov 27 2014;515(7528):563-7. doi:10.1038/nature14011

- 66. Gou Q, Dong C, Xu H, et al. PD-L1 degradation pathway and immunotherapy for cancer. *Cell Death & Disease*. 2020/11/06 2020;11(11):955. doi:10.1038/s41419-020-03140-2
- 67. Shen N, Yang C, Zhang X, Tang Z, Chen X. Cisplatin nanoparticles possess stronger antitumor synergy with PD1/PD-L1 inhibitors than the parental drug. *Acta Biomaterialia*. 2021/11/01/2021;135:543-555. doi:https://doi.org/10.1016/j.actbio.2021.08.013
- 68. Sato H, Niimi A, Yasuhara T, et al. DNA double-strand break repair pathway regulates PD-L1 expression in cancer cells. *Nature Communications*. 2017/11/24 2017;8(1):1751. doi:10.1038/s41467-017-01883-9
- 69. Nakamura K, Karmokar A, Farrington PM, et al. Inhibition of DNA-PK with AZD7648 Sensitizes Tumor Cells to Radiotherapy and Induces Type I IFN-Dependent Durable Tumor Control. *Clinical Cancer Research*. 2021;27(15):4353-4366. doi:10.1158/1078-0432.Ccr-20-3701 Shaheen FS. Znoiek P. Fisher A, et al. Targeting the DNA Double Strand Break Repair
- 70. Shaheen FS, Znojek P, Fisher A, et al. Targeting the DNA Double Strand Break Repair Machinery in Prostate Cancer. *PLOS ONE*. 2011;6(5):e20311. doi:10.1371/journal.pone.0020311
- 71. Willmore E, de Caux S, Sunter NJ, et al. A novel DNA-dependent protein kinase inhibitor, NU7026, potentiates the cytotoxicity of topoisomerase II poisons used in the treatment of leukemia. *Blood*. 2004;103(12):4659-4665. doi:10.1182/blood-2003-07-2527
- 72. Chou T-C, Talalay P. Quantitative analysis of dose-effect relationships: the combined effects of multiple drugs or enzyme inhibitors. *Advances in Enzyme Regulation*. 1984/01/01/1984;22:27-55. doi:https://doi.org/10.1016/0065-2571(84)90007-4
- 73. Weitsman G, Nuo En Chan J, Nedbal J, et al. Small molecule PD-L1 inhibitor modulates expression of PD-L1 on the cell surface a potential mechanism of blocking interaction with PD-1. *European Journal of Cancer*. 2022;174:S70. doi:10.1016/S0959-8049(22)00989-3

- 74. Powell SN, Kachnic LA. Roles of BRCA1 and BRCA2 in homologous recombination, DNA replication fidelity and the cellular response to ionizing radiation. *Oncogene*. 2003/09/01 2003;22(37):5784-5791. doi:10.1038/sj.onc.1206678
- 75. Zhang N, Li J, Gao W, et al. Co-Delivery of Doxorubicin and Anti-PD-L1 Peptide in Lipid/PLGA Nanocomplexes for the Chemo-Immunotherapy of Cancer. *Molecular Pharmaceutics*. 2022/09/05 2022;19(9):3439-3449. doi:10.1021/acs.molpharmaceut.2c00611
- 76. Ariza A, Garzon D, Abánades DR, et al. Protein haptenation by amoxicillin: High resolution mass spectrometry analysis and identification of target proteins in serum. *Journal of Proteomics*. 2012/12/21/2012;77:504-520. doi:https://doi.org/10.1016/j.jprot.2012.09.030
- 77. Zecha J, Bayer FP, Wiechmann S, et al. Decrypting drug actions and protein modifications by dose- and time-resolved proteomics. *Science*. 2023;380(6640):93-101. doi:doi:10.1126/science.ade3925
- 78. Li C-W, Lim S-O, Xia W, et al. Glycosylation and stabilization of programmed death ligand-1 suppresses T-cell activity. *Nature Communications*. 2016/08/30 2016;7(1):12632. doi:10.1038/ncomms12632
- 79. Nachmias B, Schimmer AD. Targeting nuclear import and export in hematological malignancies. *Leukemia*. Nov 2020;34(11):2875-2886. doi:10.1038/s41375-020-0958-y
- 80. Dylgjeri E, Knudsen KE. DNA-PKcs: A Targetable Protumorigenic Protein Kinase. *Cancer Research*. 2021;82(4):523-533. doi:10.1158/0008-5472.Can-21-1756
- 81. Hu X, Zhu H, Chen B, et al. Tubulin Alpha 1b Is Associated with the Immune Cell Infiltration and the Response of HCC Patients to Immunotherapy. *Diagnostics*. 2022;12(4):858.

- 82. Furnish M, Boulton DP, Genther V, et al. MIRO2 Regulates Prostate Cancer Cell Growth via GCN1-Dependent Stress Signaling. *Mol Cancer Res.* Apr 1 2022;20(4):607-621. doi:10.1158/1541-7786.Mcr-21-0374
- 83. Feng Y, Madungwe NB, Bopassa JC. Mitochondrial inner membrane protein, Mic60/mitofilin in mammalian organ protection. *J Cell Physiol*. Apr 2019;234(4):3383-3393. doi:10.1002/jcp.27314
- 84. Rulina AV, Mittler F, Obeid P, et al. Distinct outcomes of CRL–Nedd8 pathway inhibition reveal cancer cell plasticity. *Cell Death & Disease*. 2016/12/01 2016;7(12):e2505-e2505. doi:10.1038/cddis.2016.395
- 85. Tan KT, Yeh CN, Chang YC, et al. PRKDC: new biomarker and drug target for checkpoint blockade immunotherapy. *J Immunother Cancer*. Mar 2020;8(1)doi:10.1136/jitc-2019-000485
- 86. Xue Z, Zheng S, Linghu D, et al. PD-L1 deficiency sensitizes tumor cells to DNA-PK inhibition and enhances cGAS-STING activation. *Am J Cancer Res*. 2022;12(5):2363-2375.
- 87. Liu J, Li Z, Zhao D, et al. Immunogenic cell death-inducing chemotherapeutic nanoformulations potentiate combination chemoimmunotherapy. *Materials & Design*. 2021/04/01/2021;202:109465. doi:https://doi.org/10.1016/j.matdes.2021.109465

APPENDIX

Table S1: Proteomic analysis of SAOS-2 total spectrum count.

ID	W	Α	В
MYH9	227	286	240
MYH10	229	58	47
MYH14	228	38	30
FLNA	281	87	101
FLNB	278	0	0
FLNC	291	0	0
EF1A1	50	56	42
EF1A2	50	31	20
ANXA2	39	75	60
EF1G	50	58	49
RS11	18	38	29
NUCL	77	63	50
RS4X	30	31	29
HS90A	85	9	24
HS90B	83	8	23
RS2	31	20	19
PHB	30	25	33
TBA1B	<mark>50</mark>	0	<mark>65</mark>
RS3	27	29	26
RS9	23	23	19
EZRI	69	34	27
RS3A	30	12	15
MOES	68	16	20
RS7	22	27	17
MYL6	17	17	8
SYEP	171	29	23
PHB2	33	16	8
RS19	16	13	17
RS18	18	12	13
RS16	16	8	6
RSSA	33	7	3
HMGB1	25	19	10
HGB1A	24	0	0
SP100	100	15	6

<mark>PRKDC</mark>	<mark>469</mark>	0	<mark>27</mark>
RS13	17	10	8
SEPT2	41	14	10
RL7A	30	15	18
EF1D	31	18	21
S10AA	11	10	15
RS25	14	7	5
SMC4	147	6	6
DDX1	82	9	9
SEP11	49	7	6
SEPT8	56	7	4
H2B1B	14	17	6
CCD87	96	3	0
ML12A	20	8	8
MYL9	20	7	7
RS26	13	10	2
RS5	23	3	4
SRSF2	25	13	9
MCM3	91	13	9
SRP14	15	16	13
K2C1	66	1	1
ACTA	42	5	3
ADT2	33	3	11
EF1B	25	8	13
IF2A	36	11	14
RL8	28	9	8
HSP7C	71	12	16
HSP72	70	7	11
GRP78	72	3	0
TOP2A	174	7	7
RL3	46	8	7
EIF3E	52	13	9
SEPT7	51	12	10
SPTN5	417	1	1
TBB5	50	2	12
•	•		

RS15A	15	2	4
RRBP1	152	13	21
CAND1	<mark>136</mark>	0	<mark>16</mark>
GBLP	35	4	4
E41L2	113	9	15
SYIC	145	18	14
PARP1	113	15	8
H2A1C	14	6	4
H2A2B	14	0	0
SYYC	59	12	16
DYHC1	532	0	1
NPM	33	11	15
H13	22	4	6
H14	22	4	6
COCA1	333	1	1
SRCAP	344	8	14
CYFP1	145	9	5
IF2B	38	10	12
SYLC	134	20	10
HMGB2	24	8	7
H15	23	3	9
RS23	16	6	3
NAA15	101	1	9
SEPT9	65	7	4
IF2GL	51	10	7
SYQ	88	7	4
PABP1	71	7	4
PABP3	70	7	3
SYDC	57	12	7
EIF3A	167	6	7
SRP09	10	1	2
RL10A	25	8	6
EIF3F	38	4	6
RS6	29	3	7
SYK	68	8	6

SYTC	83	5	1
AP2M1	50	3	0
EXC6B	94	5	3
RL4	48	11	7
IMB1	97	3	7
RL27	16	3	2
RL26	17	4	4
PEAK1	193	6	3
ECHB	<mark>51</mark>	0	<mark>6</mark>
NEB1	123	1	1
RS10	19	4	5
POLK	99	4	3
ALBU	69	6	4
BT3L4	17	2	1
PGCB	99	3	2
MCM5	82	7	3
RS20	13	1	2
RL6	33	4	3
IQGA1	189	4	3
RLA2	12	5	3
NCKPL	128	1	0
SRCN1	112	6	3
K1C10	59	0	5
SETD2	288	7	1
RL31	14	8	5
PPIB	24	1	6
RL7	29	3	7
RS8	24	4	6
SRP54	56	7	5
CERKL	63	0	0
MACF1	838	1	3
DYST	861	1	3
UBR5	309	5	0
PDIA5	60	2	2
NAA10	26	0	2
RBM41	47	2	2
KTN1	156	7	3
ODB2	53	4	0
ATD3B	73	1	3

SRGP3	125	2	3
AIMP1	34	2	1
EIF3B	92	0	2
RL34	13	1	2
XPO2	<mark>110</mark>	0	8
IPO5	<mark>124</mark>	0	<mark>3</mark>
CFA36	39	1	1
DMD	427	0	2
RL13A	24	1	1
HNRPU	91	3	3
SRP72	75	3	4
NUCKS	27	4	3
RPN2	69	1	0
CKAP5	226	4	3
ELL2	72	2	2
ABCF3	80	8	1
S10A6	10	0	6
TFB2M	45	2	0
CROCC	229	0	2
RL13	24	2	2
RL11	20	1	4
NUA4L	10	4	1
CUL4B	104	1	4
RL23	15	1	3
AIMP2	35	4	1
AP2B1	105	0	1
NPAS2	92	2	4
TTC28	271	0	0
SNX31	51	5	0
LSM10	14	0	6
RL12	18	0	2
HNRPQ	70	2	2
RS14	16	2	2
MRT4	28	1	1
MYO1B	132	2	2
GCN1L	<mark>293</mark>	0	<mark>3</mark>
SYRC	75	3	2
H4	11	2	3
STT3A	81	0	2

MPCP	40	0	4
XPO1	<mark>123</mark>	0	<mark>3</mark>
LRMP	62	0	0
TOP1	91	3	1
UBE2O	141	3	0
ZN212	55	0	2
ABCD3	75	0	1
AP2A1	108	0	1
WEE2	63	0	1
H31T	16	4	1
NMT2	57	0	2
CNTN3	113	2	2
ILF3	95	0	1
CH60	61	0	6
XPO5	<mark>136</mark>	0	<mark>4</mark>
LPPRC	158	1	1
ULK2	113	0	0
MY18B	285	2	1
MBNL1	42	0	0
PAQR4	29	0	0
GBA3	54	0	0
S61A1	52	0	4
RS30	7	1	1
LRC59	35	0	1
CSK21	45	1	1
RS24	15	0	0
UFM1	9	0	0
ATS18	135	3	0
NPT2C	64	0	0
RL9	22	1	0
ODO2	49	2	1
DDX21	87	2	1
CLHC1	67	1	1
SMC1A	143	1	2
JMJD6	46	0	1
RUXGL	9	2	0
RL35A	13	2	0
SPERT	52	0	1
EIF3L	67	2	1

VDAC1	31	0	3
MIC60	<mark>84</mark>	0	<mark>4</mark>
ATPA	60	0	3
DNJA1	45	5	0
MYOME	265	1	0
CLPT1	76	0	5
S45A2	58	2	1
SPC1L	38	1	3
EIF3I	37	0	3
SC31B	129	0	1
TPX2	86	0	1
ACTN4	105	0	1

SYDM	74	0	3
ITA9	114	3	2
AT2A3	114	0	2
F120S	28	3	0
FMN1	158	1	2
LAMB2	196	0	1
UTF1	36	3	0
PA2G4	44	0	1
RLA1	12	1	1
SURF4	30	0	1
RS28	8	1	1
RL35	15	2	1

59	2	0
71	2	1
55	1	1
88	1	0
<mark>120</mark>	0	<mark>4</mark>
41	0	1
99	0	2
57	1	1
40	0	1
28	2	0
	71 55 88 120 41 99 57	71 2 55 1 88 1 120 0 41 0 99 0 57 1 40 0

Proteomic data generated from the use of AB22 (A) and AF147 (B). Accession number (ID) refers to the unique identifier given to a protein in sequence databases. Molecular weight (W) is reported in kDa. Proteins highlighted in yellow are identified as binding partners of AF147.

Table S2: Proteomic analysis of A549 WT total spectrum count.

ID	W	Α	В
MYH9	227	88	227
MYH14	228	17	24
EF1A1	50	149	64
EF1A2	50	110	41
ANXA2	39	99	81
PRKDC	<mark>469</mark>	0	<mark>200</mark>
TOP2A	174	89	89
MYH10	229	23	91
EF1G	50	87	65
RS4X	30	40	51
RS3	27	61	35
RS9	23	60	29
EIF3A	167	25	109
SYEP	171	33	78
SYIC	145	33	90
RS3A	30	49	40
PHB	30	22	35
RS11	18	43	23

RS2	31	44	29
RS16	16	52	17
SYDC	57	35	59
PHB2	33	33	32
IF2A	36	33	42
NUCL	77	33	53
EF1D	31	36	36
RS7	22	30	24
TOP2B	183	35	59
DDX21	87	36	51
RS13	17	45	24
KTN1	156	5	96
GCN1L	<mark>293</mark>	0	<mark>100</mark>
RS19	16	25	23
RSSA	33	30	25
ACTB	42	9	25
SYLC	134	23	68
SYK	68	19	44
SYK RS18	68 18	19 34	44 19

IF2B	38	15	42
HS90A	85	10	47
FLNA	281	0	55
FLNC	291	0	0
FLNB	278	0	0
H13	22	36	26
H14	22	35	26
H12	21	0	0
EZRI	69	3	49
MOES	68	2	32
RADI	69	0	20
GBLP	35	30	15
HSP7C	71	2	52
MAP1B	271	2	75
SYQ	88	13	53
SYRC	75	4	62
EIF3B	92	14	49
AHNK	629	4	83
EIF3E	52	17	26

6	57
	٠,
14	34
6	33
6	30
0	18
0	0
1	43
0	0
10	57
0	0
23	15
0	71
0	4
10	59
20	23
27	5
17	0
0	56
0	<mark>35</mark>
3	19
13	39
14	40
9	22
9	20
0	0
6	31
11	14
23	26
13	34
0	0
0	<mark>51</mark>
10	17
6	36
6	34
6	27
20	13
17	9
5	35
9	22
	6 6 0 0 1 0 10 0 23 0 0 10 20 27 17 0 0 3 13 14 9 9 0 6 11 23 0 0 0 10 0 10 0 10 10 10 10 10 10 10 10

AIMP1	34	12	27
EIF3C	105	0	46
SYMC	101	13	34
SP16H	120	11	39
RS25	14	17	10
ML12A	20	1	24
RL8	28	11	15
MYL6	17	5	16
PRDX1	<mark>22</mark>	0	<mark>25</mark>
RL27	16	15	8
DNJA1	45	3	17
RS23	16	7	12
AIMP2	35	4	7
NOLC1	74	7	31
NAA15	101	0	32
PPIB	24	2	27
CYFP1	145	0	22
XPO1	<mark>123</mark>	0	<mark>38</mark>
RS26	13	9	9
HS71A	70	0	24
RL9	22	9	16
EIF3I	37	5	25
S10AA	11	6	12
DDX50	83	18	11
LACTB	61	0	28
MCM5	82	3	24
RS6	29	3	10
RL7	29	2	23
EIF3G	36	16	15
IF2P	139	0	40
SRP54	56	0	27
ASPH	86	0	28
MBB1A	149	6	30
SYVC	140	0	36
SDCB1	32	9	8
SPTN5	417	15	0
GRP78	<mark>72</mark>	0	<mark>29</mark>
RS14	16	1	15
HMGB1	25	0	30
		1	

SP100	100	0	0
CKAP5	226	0	31
RS8	24	6	15
SQSTM	48	0	19
EIF3D	64	0	30
RL26	17	9	9
SRSF2	25	10	11
RS17	16	1	10
IMB1	97	0	21
RLA0	34	0	17
RLA0L	34	0	15
EIF3H	40	0	25
CCD87	96	15	0
RS20	13	3	13
SSRP1	81	2	19
RL5	34	1	20
RL13A	24	10	10
TBA4B	28	0	8
PGAP1	105	8	0
RUVB1	50	0	24
SMC3	142	0	34
SMC1A	143	0	29
RL10A	25	9	11
RL34	13	6	8
PRP8	274	0	25
XPO2	<mark>110</mark>	0	<mark>24</mark>
MROH8	55	10	1
MCM3	91	0	21
RLA2	12	8	5
SEP11	49	0	14
SEPT8	56	0	0
SEPT7	51	0	17
TERA	89	0	17
SRP68	71	0	20
AP3B1	121	0	28
RUVB2	51	0	23
RL23	15	2	8
RL1D1	55	6	11
SRCAP	344	8	1

SEPT2	41	0	5
IPO7	<mark>120</mark>	0	<mark>20</mark>
CH60	61	0	15
NEB1	123	8	0
RL13	24	4	9
RS24	15	2	11
PEAK1	193	9	2
IF5	49	1	18
SMCA1	123	0	21
SMCA5	122	0	13
SRP72	75	0	20
ITA10	128	11	0
RL31	14	4	6
CSK21	45	6	8
MPCP	40	0	16
ALBU	69	0	4
VIGLN	141	0	18
RAD50	154	0	21
RL23A	18	1	12
NAA10	26	0	11
RL35	15	5	5
RL35A	13	6	8
GRP75	74	0	7
NAT10	116	0	20
TCOF	152	0	18
RL12	18	4	7
RTCB	55	0	13
RL28	16	1	11

SRP14	15	1	10
VDAC2	32	0	11
HSPB1	23	0	15
NPT2A	69	1	1
DDX24	96	0	18
LRC59	35	0	10
SYTC	83	0	5
K1C10	59	2	4
IPO5 [2]	124	0	18
IPO5	<mark>124</mark>	0	<mark>18</mark>
RNBP6	125	0	0
NCKP1	129	0	13
UBE2O	141	0	13
RS29	7	0	13
YBOX1	36	0	13
KRT81	55	0	17
TCRG1	124	0	20
THOC2	183	0	19
RL10	25	0	9
AP2M1	50	0	8
RL15	24	0	11
MTNA	39	4	0
RL18	22	0	11
ATPA	60	0	6
RU17	52	3	12
HMGB2	24	0	11
MYO1B	132	0	14
MYO1A	118	0	0

NPM	33	1	11
SART3	110	0	14
AT2A2	115	0	14
LC7L2	47	0	11
LUC7L	44	0	8
SEPT9	65	0	8
U2AF2	54	2	8
RL32	16	1	7
RS15	17	0	5
H15	23	2	11
ERLN1	39	0	9
NAMPT	56	0	14
AT10B	165	6	0
RS27 [2]	9	0	11
RS27	9	0	9
RS27L	9	0	4
ERLN2	38	0	11
MIC19	26	0	12
UBF1	89	0	17
ALAT2	58	0	0
RS10	19	3	5
RPN1	69	0	10
SRP09	10	4	8
HSP7E	55	0	9
EXC6B	94	5	0
NMT2	57	6	0

Proteomic data generated from the use of AB22 (A) and AF147 (B). Accession number (ID) refers to the unique identifier given to a protein in sequence databases. Molecular weight (W) is reported in kDa. Proteins highlighted in yellow are identified as binding partners of AF147.